# Reaction Diffusion Model of the Enzymatic Erosion of Insoluble Fibrillar Matrices

Abraham R. Tzafriri,*[#] Michel Bercovier,* and Hanna Parnas[#]

*School of Computer Science and Engineering, and [#]The Otto Loewi Minerva Center for Cellular and Molecular Neurobiology, Department of Neurobiology, Jerusalem 91904, Israel

ABSTRACT    Predicting the time course of in vivo biodegradation is a key issue in the design of an increasing number of biomedical applications such as sutures, tissue analogs and drug-delivery devices. The design of such biodegradable devices is hampered by the absence of quantitative models for the enzymatic erosion of solid protein matrices. In this work, we derive and simulate a reaction diffusion model for the enzymatic erosion of fibrillar gels that successfully reproduces the main qualitative features of this process. A key aspect of the proposed model is the incorporation of steric hindrance into the standard Michaelis–Menten scheme for enzyme kinetics. In the limit of instantaneous diffusion, the model equations are analogous to the standard equations for enzymatic degradation in solution. Invoking this analogy, the total quasi-steady-state approximation is used to derive approximate analytical solutions that are valid for a wide range of in vitro conditions. Using these analytical approximations, an experimental–theoretical method is derived to unambiguously estimate all the kinetic model parameters. Moreover, the analytical approximations correctly describe the characteristic hyperbolic dependence of the erosion rate on enzyme concentration and the zero-order erosion of thin fibers. For definiteness, the analysis of published experimental results of enzymatic degradation of fibrillar collagen is demonstrated, and the role of diffusion in these experiments is elucidated.

## INTRODUCTION

Enzymatic degradation of fibrillar collagen networks is a fundamental process in connective tissue remodeling. An understanding of the mechanism of the degradation process is also of great importance in a host of biodegradable biomedical devices such as connective tissue analogs (Chamberlain et al., 1997; Sung et al., 1997; Compton et al., 1998; Riesle et al., 1998; Freyman et al., 2001), sutures (Hayashi et al., 1990; Okada et al., 1992), vascular grafts (Van Wachem, et al., 2001), drug-delivery devices (Gilbert and Kim, 1990; Freiss et al., 1996; Freiss, 1998; Fujioka et al., 1998; Wissink et al., 2000), etc. (Sabelman, 1985; Li, 1995; Nimni, 1995), as well as in processing of wood and cellulosic fibers (Viikari et al., 1991). Under in vivo and in vitro conditions, collagen aggregates into a network of approximately cylindrical fibrils with diameters varying between 20 and 500 nm, according to collagen age, type, composition, and tissue source (Stryer, 1988; Kadler et al., 1996; Riesle et al., 1998). Degradation of collagen monomers (i.e., tropocollagen) in solution by specific and nonspecific collagenases has been shown to follow Michaelis–Menten kinetics (Welgus et al., 1981a,b, 1982; Van Wart and Steinbrink, 1985; Mallya et al., 1992). In contrast, the degradation of fibrillar collagen depends on the age of the sample, with fresh samples behaving similarly to collagen molecules in solution, and older samples behaving anomalously with respect to enzyme concentration (Steven, 1976a,b). Namely, the erosion rate of mature fibrillar samples has been shown to depend hyperbolically on enzyme concentrations, even when the number of collagen monomers is greatly in excess of the number of enzyme molecules (Steven, 1976a,b; Welgus et al., 1980). Because this behavior is observed both with vertebrate collagenase and bacterial collagenase (and even with trypsin), it has been suggested that these anomalies are related to the microstructure of fibrillar collagen, namely to steric exclusion of the large enzyme molecules from the bulk of the fibrils due to very tight packing. Although this interpretation is widely accepted, and has been used to intuitively rationalize the experimental observations (Steven, 1976; Welgus et al., 1980), the implications of steric obstruction of enzyme binding sites on the transient degradation have not been explored quantitatively.

To date, except for the work of Suga et al. (1975), most mathematical modeling of enzymatic erosion of insoluble protein fibers has been of an ad hoc phenomenological nature. Hayashi and Ikada (1990) suggested that enzymatic erosion of insoluble polymer fibers is a pure surface erosion process and derived a simple model based on the assumption that the radius of the fiber decreases linearly with time. This model implies that the square root of the fiber mass decreases linearly with time, and seems to be consistent with most of the experimental data obtained by Okada et al. (1992) regarding the erosion of cross-linked collagen fibers by bacterial collagenase at 37°C. Although the assumption of surface erosion seems plausible for large enzymes, no justification was given for the assumption that the fiber radius decreases linearly with time.

Bailey and Ollis (1977) reanalyzed published data on the enzymatic erosion of insoluble proteins and demonstrated that the rate of erosion depends hyperbolically on enzyme concentration. They explained this hyperbolic dependence by suggesting that Langmuir surface adsorption is the rate-limiting step in the hydrolysis of insoluble enzyme. Although plausible, this explanation overlooks the fact that the Langmuir adsorption isotherm is used to describe adsorption of proteins onto non-

eroding surfaces (Letnam, 1951) and its applicability for eroding surfaces is questionable. Thus, although Sattler et al. (1989) were able to fit the initial rate of enzymatic hydrolysis of cellulose to a Langmuir adsorption isotherm, the resulting binding constant was found to be time dependent.

In this work, we derive a reaction diffusion model for the enzymatic erosion of insoluble fibrillar matrices that takes into account two inherent heterogeneities: 1) the macroscopic heterogeneity of the gel–solution system, which entails that we consider the diffusion of the enzyme into the sample and the diffusion of the degradation products out of the sample (Suga et al., 1975), and 2) the confinement of the binding sites available for the enzyme to the surface of the fibrils, which is translated into a novel kinetic scheme. The limit of instantaneous diffusion of this model is derived and studied using the quasi-steady-state approximation (QSSA). The latter approximation allows us to derive a closed-form approximation for the rate of degradation that is valid for a wide range of model parameters, and which can explain the success of the ad hoc correlations of previous researchers (Bailey and Ollis, 1977; Hayashi and Ikada, 1990). Moreover, the QSSA enables us to identify the model parameters (basic or composite) that govern the transient degradation under different experimental conditions and suggests an experimental–theoretical method of estimating these parameters. The limit of instantaneous diffusion is shown to be roughly valid for the experiments of Welgus et al. (1980) on the in vitro erosion of fibrillar collagen by matrix fibroblast collagenase at 37°C. Although those experiments are only partially consistent with the theoretical–experimental method proposed in the current paper, the QSSA is shown to be roughly valid for them and enables us to estimate the Michaelis–Menten constant of that system, which could not be assessed before. Using this estimate to simulate additional erosion experiments (Welgus et al., 1980), elucidates the role of diffusion. Moreover, the consistency between simulation and experiment reinforces the validity of the proposed model and the parameter estimates obtained in this work.

## MATHEMATICAL MODEL

### Overview

Here we derive a model for the erosion of an insoluble fibrillar matrix (e.g., collagen gel) by a specific enzyme that has a single cleavage site on the monomer of which the fibril is composed (e.g., skin fibroblast collagenase). The fibrillar gel is modeled as a solid porous network immersed in a buffered enzyme solution. The fibrils are idealized as perfect cylinders of tightly packed monomeric rods (see Fig. 1). This idealization is a good approximation as long as the fibril diameter, $d_f$, is much larger than the diameter of the monomer, $d_m$. When this network comes in contact with the enzyme solution, the enzyme diffuses into the gel where it binds to specific sites on monomers located at the surface of the fibrils. Due to their size, the enzyme molecules cannot
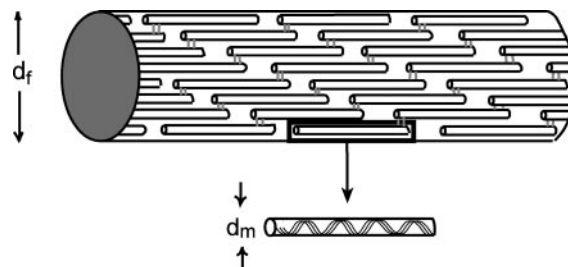


FIGURE 1  Schematics of an idealized cylindrical fibril segment composed of many tightly packed cross-linked monomers that are modeled as rigid rods. The blowup depicts a single monomeric subunit. The diameter of the fibril, $d_f$, is much larger than the diameter of its cylindrical monomeric subunits, $d_m$.

penetrate the tightly packed (cross-linked) monomers that make up an individual fibril. This problem is inherently heterogeneous, because the reaction is confined to the gel.

A crucial simplifying assumption in the subsequent derivation is that cleavage is the rate-limiting step of fibril erosion (e.g., as in fibrillar collagen at T > 35°C (Sakai and Gross, 1967; Welgus et al. 1980)). Thus, once a monomer at the surface of a fibril is cleaved, it is assumed to spontaneously detach and go into the solution, where it diffuses, eventually reaching the gel–liquid interface. This assumption will enable us to use standard enzyme kinetics for the degradation process at the surface of the fibrils (Lin et al., 1999), and moreover implies that fibril erosion is confined to its surface.

### Basic kinetic scheme

The reaction between the enzyme and monomer substrate is assumed to be of the common Michaelis–Menten type (Stryer, 1988; Suga et al., 1975; Lin et al., 1999)

$$E + \rho \underset{k_r}{\overset{\bar{k}_f}{\leftrightarrow}} C \overset{k_{cat}}{\longrightarrow} E + P. \tag{1}$$
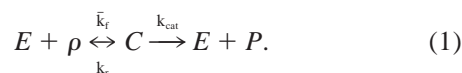
Here $E$ and $C$ denote the free and bound enzyme (inside the matrix), respectively, $\rho$ denotes the substrate (monomer) and $P$ denotes the degradation products (i.e., the cleared monomers), $\bar{k}_f$ is the rate constant of formation (per unit substrate) of the enzyme–substrate complex, $k_r$ is the rate constant of dissociation of the enzyme substrate complex, and $k_{cat}$ is the catalysis rate. The final step in kinetic scheme 1 is irreversible because the enzyme only catalyzes the degradation of the monomers. Moreover, because we assume that cleaved monomers detach spontaneously and go into solution, association of cleaved monomers is expected to be negligible.

Kinetic scheme 1 implies the following kinetic equations for the immobilized species in the gel matrix:

$$\frac{\partial \rho}{\partial t} = -\bar{k}_f E \rho + k_r C, \tag{2}$$

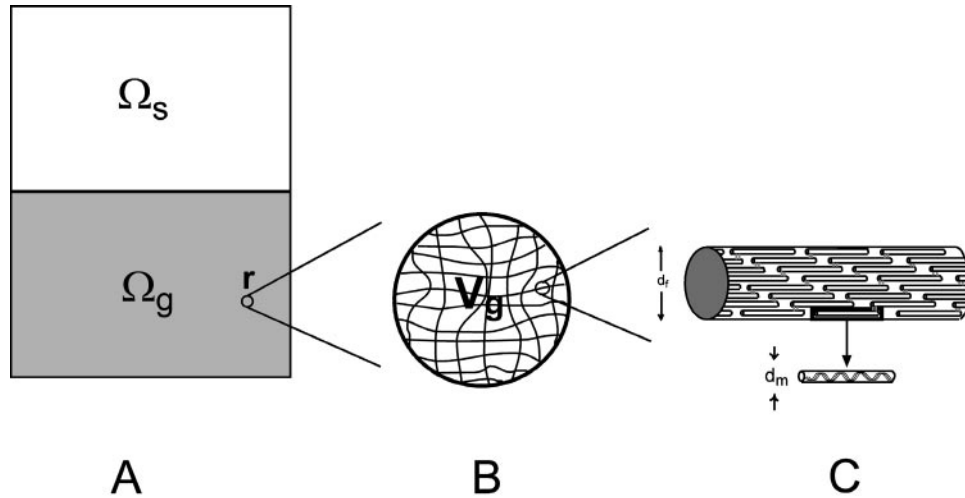$$\frac{\partial C}{\partial t} = \bar{k}_f E \rho - (k_r + k_{cat}) C, \tag{3}$$

FIGURE 2 Multiscale geometry of the problem. (A) Schematics of the (macroscopic) gel matrix ($\Omega_g$) and the surrounding solution layer ($\Omega_s$). (B) Blowup of a (mesoscopic) region of volume $V_g$ around a point $\mathbf{r} \in \Omega_g$. (C) Blowup of a typical fibril segment in $V_g$ revealing its microscopic structure.

and the following reaction–diffusion equations for the mobile species in the gel matrix (Crank, 1975):

$$\frac{\partial E}{\partial t} - \nabla \cdot (D_{e,g} \nabla E) = -\frac{\partial C}{\partial t}, \quad (4)$$

$$\frac{\partial P}{\partial t} - \nabla \cdot (D_{p,g} \nabla P) = k_{cat} C, \quad (5)$$

where $D_{e,g}$ and $D_{p,g}$ are, respectively, the diffusion coefficient of the free enzyme and the degradation products inside the gel matrix. Denoting the concentration (per unit volume) of available (unoccupied) binding sites (i.e., attached monomers) on the surface of the fibrils by $S$, we note that $\bar{k}_f$ has to satisfy the relation,

$$\bar{k}_f \rho \equiv k_f S, \quad (6)$$

where $k_f$ is the rate of complex formation per available substrate molecule. Eq. 6 is a manifestation of the fact that the available binding sites are all located at the surface of the fibrils. Thus, whereas $k_f$ is a basic (constant) parameter of the system, the effective reaction parameter $\bar{k}_f$ is a variable proportional to the ratio $S/\rho$. Substituting Eq. 6 into Eqs. 2 and 3, we obtain

$$\frac{\partial \rho}{\partial t} = -k_f E \cdot S + k_r C$$
$$= -k_f(\bar{S} - C) + k_r C, \quad (7)$$

$$\frac{\partial C}{\partial t} = k_f E \cdot S - (k_r + k_{cat}) C$$
$$= k_f E \cdot (\bar{S} - C) - (k_r + k_{cat}) C, \quad (8)$$

where

$$\bar{S} = S + C \quad (9)$$

denotes the total concentration of surface binding sites, both free and bound. To close this system of equations, we have to relate between $\bar{S}$ and

$$\bar{\rho} = \rho + C, \quad (10)$$

the total concentration of collagen monomers. Such a relation is derived in the following section.

## Concentration of surface binding sites

Consider a (constant) reference volume $V_g(\mathbf{r})$ centered at a point labeled by the vector $\mathbf{r}$ inside the gel. This reference volume is chosen such that it is small compared to the total volume of the gel matrix, but large compared to the typical network diameter, so that it contains many fibril segments (see Fig. 2). Let $N(\mathbf{r}, t)$ and $n(\mathbf{r}, t)$, respectively, denote the total number of rod-shaped monomers of length $L_m$ and fibril segments of length $L_m$ in $V_g(\mathbf{r})$ at time $t$. As degradation proceeds, the number of fibril segments $n$ and the monomer diameter $d_m$ are constant, but the total number of monomers $N$ and the fibril diameter $d_f$ decrease.

The total molar concentration of (undegraded) monomers, $\bar{\rho}$, therefore satisfies the relations

$$\bar{\rho}(\mathbf{r}, t) = \frac{N(\mathbf{r}, t)}{V_g(\mathbf{r})}, \quad (11)$$

$$\frac{\bar{\rho}(\mathbf{r}, t)}{\rho_0} = \frac{N(\mathbf{r}, t)}{N_0}, \quad (12)$$

where $\rho_0$ and $N_0$ denote the initial values of $\bar{\rho}$ and $N$, respectively. Figure 3 shows a cross section of a typical fibril segment. The total concentration of surface binding sites, $\bar{S}$, is the product of the concentration of fibril segments
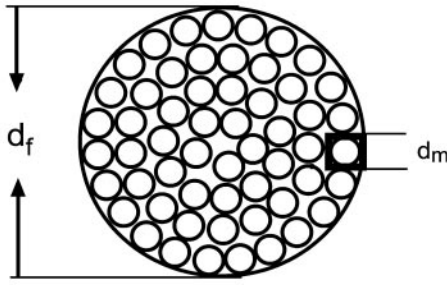
FIGURE 3 Schematics of a cross section perpendicular to the axis of the fibril. The area of such a cross section is $\pi d_f^2/4$ and is covered by many tightly packed circles (e.g., monomer cross sections) of diameter $d_m$. Because the monomers are incompressible, the circles do not overlap and are equivalent to squares of side $d_m$ in terms of coverage.

of length $L_m$, $n_0/V_g$, with the total number of monomers (e.g., circles of diameter $d_m$) on the circumference of such a cross section, $\pi d_f/d_m$, namely,

$$\bar{S}(\mathbf{r}, t) = \frac{\pi n_0}{V_g(\mathbf{r})} \frac{d_f(\mathbf{r}, t)}{d_m}. \tag{13}$$

The area of the cross section depicted in Fig. 3 is $\pi d_f^2/4$ and it is covered by tightly packed circles (e.g., monomer cross sections) of diameter $d_m$. Because the monomers are incompressible, the circles do not overlap and are equivalent to squares of side $d_m$ in terms of coverage. Equating the total volume of fibril segments in $V_g(\mathbf{r})$, $n_0 L_m(\pi d_f^2/4)$, to the total equivalent volume of monomers in $V_g(\mathbf{r})$, $N L_m d_m^2$, we obtain

$$N(\mathbf{r}, t) = \frac{\pi n_0}{4} \left(\frac{d_f(\mathbf{r}, t)}{d_m}\right)^2 \tag{14}$$

and

$$\frac{\bar{\rho}(\mathbf{r}, t)}{\rho_0} = \frac{N(\mathbf{r}, t)}{N_0} = \left(\frac{d_f(\mathbf{r}, t)}{d_f(\mathbf{r}, 0)}\right)^2. \tag{15}$$

Sequential application of Eqs. 11 and 14 yields

$$\frac{\pi n_0}{V_g(\mathbf{r})} = \frac{n_0 \pi}{N_0} \rho_0 = \left(\frac{d_m}{d_f(0)}\right)^2 4\rho_0. \tag{16}$$

Substituting the latter result into Eq. 13, and using Eq. 15 to further simplify, yields

$$\bar{S}(\mathbf{r}, t) = \frac{4\rho_0 d_m}{d_f(0)} \frac{d_f(\mathbf{r}, t)}{d_f(0)}$$

$$= \frac{4\rho_0 d_m}{d_f(0)} \left(\frac{\bar{\rho}(\mathbf{r}, t)}{\rho_0}\right)^{1/2}$$

$$= \kappa \bar{\rho}^{1/2}(\mathbf{r}, t), \tag{17}$$

where the proportionality constant $\kappa$ is defined as

$$\kappa \equiv \frac{4 d_m}{d_f(0)} \rho_0^{1/2}. \tag{18}$$

Initially we have

$$\bar{S} = \kappa \rho_0^{1/2} = \gamma \rho_0, \quad t = 0, \tag{19}$$

where

$$\gamma \equiv \frac{4 d_m}{d_f(0)}. \tag{20}$$

Recall that the results of this section were obtained by approximating the fibril as a cylinder with a smooth surface and are only valid provided that $d_m \ll d_f$. For fibrillar collagen, $d_m \approx 1.5$ nm and $22$ nm $\leq d_f(0) \leq 500$ nm (Hulmes et al., 1995). This implies that the approximations of this section should always be roughly valid at least during the initial stages of fibrillar collagen degradation.

## The reaction diffusion equations

Incorporating result 17 into Eqs. 7 and 8, we obtain

$$\frac{\partial \rho}{\partial t} = -k_f E(\kappa \bar{\rho}^{1/2} - C) + k_r C, \quad \mathbf{r} \in \Omega_g, \tag{21}$$

$$\frac{\partial C}{\partial t} = k_f E(\kappa \bar{\rho}^{1/2} - C) - (k_r + k_{cat})C, \quad \mathbf{r} \in \Omega_g. \tag{22}$$

$$\frac{\partial E}{\partial t} - \nabla \cdot (D_{e,g} \nabla E) = \frac{\partial C}{\partial t}, \quad \mathbf{r} \in \Omega_g, \tag{23}$$

$$\frac{\partial P}{\partial t} - \nabla \cdot (D_{p,g} \nabla P) = k_{cat} C, \quad \mathbf{r} \in \Omega_g. \tag{24}$$

Here, $\Omega_g$ denotes the gel matrix, and we remind the reader that $\bar{\rho} = \rho + C$. Because $\bar{\rho}$ appears naturally in Eq. 22, it is convenient to replace Eq. 21 by a rate equation for $\bar{\rho}$. This is achieved by adding Eqs. 21 and 22, to obtain

$$\frac{\partial \bar{\rho}}{\partial t} = -k_{cat} C. \tag{25}$$

In this work, we consider the uniform initial conditions,

$$\bar{\rho} = \rho_0, \quad t = 0 \quad \text{and} \quad \mathbf{r} \in \Omega_g, \tag{26}$$

$$P = C = E = 0, \quad t = 0 \quad \text{and} \quad \mathbf{r} \in \Omega_g. \tag{27}$$

As (standard) boundary conditions, we impose continuity of the fluxes across the gel–liquid interface (denoted as $\partial\Omega_g$)

$$-D_{e,g} \nabla E = -D_{e,s} \nabla E_s, \quad \mathbf{r} \in \partial\Omega_g, \tag{28}$$

$$-D_{p,g} \nabla P = -D_{p,s} \nabla P_s, \quad \mathbf{r} \in \partial\Omega_g, \tag{29}$$

where $E_s$ and $P_s$ denote the concentrations of free enzyme and degradation products in the surrounding solution layer,

respectively, and $D_{e,s}$, $D_{p,s}$ are the corresponding diffusion coefficients. Because the enzymatic reaction is confined to the gel, the dynamics of the free enzyme and the degradation products in the surrounding liquid layer are described by the equations,

$$\frac{\partial E_s}{\partial t} - D_{e,s}\Delta E_s = 0, \quad \mathbf{r} \in \Omega_s, \qquad (30)$$

$$\frac{\partial P_s}{\partial t} - D_{p,s}\Delta P_s = 0, \quad \mathbf{r} \in \Omega_s, \qquad (31)$$

$$E_s = E_{s0}, \qquad t = 0 \quad \text{and} \quad \mathbf{r} \in \Omega_s, \qquad (32)$$

$$P_s = 0, \qquad t = 0 \quad \text{and} \quad \mathbf{r} \in \Omega_s, \qquad (33)$$

where $\Omega_s$ denotes the volume of the external solution layer.

## The low-temperature limit

The activation energies associated with the enzymatic degradation of fibrillar collagen are significantly higher than the corresponding values for degradation of tropocollagen monomers in solution (Welgus et al., 1981). The fact that enzymatic degradation of fibrillar collagen becomes negligible at 25°C and 4°C for skin fibroblast collagenase and bacterial collagenase, respectively, has enabled researchers to measure the binding of these enzymes to fibrillar collagen in the absence of significant degradation (Welgus et al., 1980; Matsushita et al., 1998). Such experiments correspond to substituting $k_{cat} \approx 0$ in Eqs. 22–33 to obtain

$$\frac{\partial C}{\partial t} = k_f E(\kappa\rho_0^{1/2} - C) - k_r C, \quad \mathbf{r} \in \Omega_g, \qquad (34)$$

$$\frac{\partial E}{\partial t} - \nabla \cdot (D_{e,g}\nabla E) = -\frac{\partial C}{\partial t}, \quad \mathbf{r} \in \Omega_g, \qquad (35)$$

$$C = E = 0, \qquad t = 0 \quad \text{and} \quad \mathbf{r} \in \Omega_g, \qquad (36)$$

$$-D_{e,g}\nabla E = -D_{e,s}\nabla E_s, \quad \mathbf{r} \in \partial\Omega_g, \qquad (37)$$

$$\frac{\partial E_s}{\partial t} - D_{e,s}\Delta E_s = 0, \quad \mathbf{r} \in \Omega_s, \qquad (38)$$

$$E_s = E_{s0}, \qquad t = 0 \quad \text{and} \quad \mathbf{r} \in \Omega_s. \qquad (39)$$

It is noteworthy that this is the standard reaction–diffusion formulation of absorption and binding of a solute by a porous matrix, with $\kappa\rho_0^{1/2} = \gamma\rho_0$ playing the role of the maximal binding capacity.

## THE LIMIT OF INSTANTANEOUS DIFFUSION

The above model of enzymatic erosion of insoluble fibrillar gels is much more complex than the Michaelis–Menten kinetic scheme that is commonly used to study enzymatic processes in solution. Namely, the proposed model depends on seven more model parameters than the standard Michaelis–Menten scheme and involves the solution of a set of coupled partial differential equations, as opposed to a set of coupled ordinary differential equations in the Michaelis–Menten model. According to Buckingham's $\Pi$ theorem (Buckingham, 1914), the number of independent dimensionless variables is equal to the number of physical quantities (e.g., model parameters) minus the number of independent physical dimensions (e.g., length and time). This implies that Eqs. 22–33 depend on ten dimensionless variables, whereas the standard Michaelis–Menten scheme depends on only three dimensionless variables. Thus, the inclusion of diffusion complicates the model significantly.

However, whenever the characteristic time scales of the diffusion of the free enzyme and degradation products in the gel and in the external solution layer are much shorter than the characteristic time for product formation, diffusion can be assumed to be instantaneous. In this case, the concentrations of the reactants and products can be assumed uniform within the gel, subject to the global enzyme conservation relation,

$$(C + E)|\Omega_g| + E_s|\Omega_s| = E_{s0}|\Omega_s|, \qquad (40)$$

where $|\Omega_g|$ and $|\Omega_s|$ are the volumes of gel and the external solution layer, respectively. This conservation relation is derived by noting that, whereas the bound enzyme is confined to the gel, the free enzyme distributes uniformly in the aqueous phase both inside the gel and in the surrounding fluid layer. For sparse gels, we can safely neglect partition and substitute $E = E_s$ in Eq. 40 to obtain

$$C|\Omega_g| + E_s V_t = E_{s0}(V_t - |\Omega_g|), \qquad (41)$$

where $V_t = |\Omega_g \cup \Omega_s|$ is the total volume of the system. Introducing the simplifying definitions

$$h \equiv V_t/|\Omega_g| \leq 1, \qquad (42)$$

$$E_0 = E_{s0}(1 - h^{-1}), \qquad (43)$$

into relation 41, we obtain

$$E = E_0 - h^{-1}C. \qquad (44)$$

To summarize, in the limit of instantaneous diffusion, our model reduces to the set of nonlinear ordinary differential equations,

$$\frac{d\bar{\rho}}{dt} = -k_{cat}C, \qquad (45)$$

$$\frac{dC}{dt} = k_f[(E_0 - h^{-1}C)(\kappa\bar{\rho}^{1/2} - C) - K_M C], \qquad (46)$$

subject to the initial conditions

$$\bar{\rho} = \rho_0, \quad t = 0, \qquad (47)$$

$$C = 0, \quad t = 0, \qquad (48)$$

and the substrate conservation relation

$$P = h^{-1}(\rho_0 - \bar{\rho})_1, \quad t = 0. \tag{49}$$

Here,

$$K_M \equiv \frac{k_r + k_{cat}}{k_f}, \tag{50}$$

is the Michaelis–Menten constant of the system. These equations are analogous to the equations describing enzymatic reactions in solution. This analogy will be exploited to derive approximate analytical solutions and parameter estimation methods.

With the exception of the low-temperature limit, Eqs. 45–48 are nonintegrable. In the low-temperature limit, $k_{cat} \approx 0$ and $\kappa\rho_0^{1/2} = \gamma\rho_0$, so that Eq. 46 takes on the form,

$$\frac{dC}{dt} = k_f[(E_0 - h^{-1}C)(\gamma\rho_0 - C) - K_D C]$$

$$= k_f h^{-1}(C - \lambda_+(\rho_0))(C - \lambda_-(\rho_0)), \tag{51}$$

where

$$K_D \equiv \frac{k_r}{k_f}, \tag{52}$$

is the Langmuir binding constant of the enzyme, and

$$\lambda_\pm(\rho_0) = \frac{1}{2}[(\gamma\rho_0 + h(E_0 + K_D))$$

$$\pm \sqrt{(\gamma\rho_0 + h(E_0 + K_D))^2 - 4hE_0\gamma\rho_0}], \tag{53}$$

are the roots of the quadratic equation,

$$C^2 - (\gamma\rho_0 + h(E_0 + K_D))C + hE_0\gamma\rho_0 = 0. \tag{54}$$

Integration of Eq. 51 yields

$$C = \lambda_-(\rho_0)\left(\frac{1 - e^{-t/\tau_C}}{1 - (\lambda_-(\rho_0)/\lambda_+(\rho_0))e^{-t/\tau_C}}\right), \tag{55}$$

where we introduced the simplifying notation,

$$\tau_C \equiv \frac{1}{k_f h^{-1}(\lambda_+(\rho_0) - \lambda_-(\rho_0))}$$

$$= \frac{h}{k_f\sqrt{(\gamma\rho_0 + h(E_0 + K_D))^2 - 4hE_0\gamma\rho_0}}. \tag{56}$$

Note that $\lambda_\pm(\rho_0) \geq 0$ and that $\lambda_-(\rho_0)$ corresponds to the steady-state concentration of bound enzyme, $C_{eq}$, as can be inferred by taking the $t \to \infty$ limit of result 55. Hence,

$$C_{eq} = \frac{1}{2}[(\gamma\rho_0 + h(E_0 + K_D))$$

$$- \sqrt{(\gamma\rho_0 + h(E_0 + K_D))^2 - 4hE_0\gamma\rho_0}], \tag{57}$$

regardless of the rate of diffusion. Namely, because this is an equilibrium result, its validity transcends that of the limit of instantaneous diffusion.

## The quasi-steady-state approximation

As already mentioned, Eqs. 45–48 are nonintegrable for $k_{cat} > 0$. However, these equations are no more complex than the equations corresponding to the standard Michaelis–Menten scheme (Stryer, 1988). The latter are also nonintegrable but have been successfully analyzed using the QSSA (Segel and Slemrod, 1989; Borghans et al., 1996; Schnell and Mendoza, 1997; Schnell and Maini, 2000). Below, we derive the QSSA corresponding to Eqs. 45–48 and analyze its validity using a modification of the procedure described by Borghans et al. (1996).

### The total QSSA

The dynamics of the enzyme–substrate complex is best analyzed by rewriting Eq. 46 as

$$\frac{dC}{dt} = k_f h^{-1}(C - C_+(\bar{\rho}))(C - C_-(\bar{\rho})), \tag{58}$$

where

$$C_\pm(\bar{\rho}) = \frac{1}{2}[(\kappa\bar{\rho}^{1/2} + h(E_0 + K_M))$$

$$\pm \sqrt{(\kappa\bar{\rho}^{1/2} + h(E_0 + K_M))^2 - 4hE_0\kappa\bar{\rho}^{1/2}}], \tag{59}$$

are the roots of the quadratic equation,

$$C^2 - (\kappa\bar{\rho}^{1/2} + h(E_0 + K_M))C + hE_0\kappa\bar{\rho}^{1/2} = 0. \tag{60}$$

The analogy with Eq. 51 is obvious and suggests that, for a given value of $\bar{\rho}$ the concentration of the enzyme–substrate complex tends to the quasi-steady-state value $C_-(\bar{\rho})$. However, $\bar{\rho}$ is not constant, and Eqs. 45 and 46 cannot be solved analytically. We shall therefore proceed to find analytical approximations for the initial transient and the subsequent quasi-steady state.

Initial conditions 47 and 48 imply that, during the initial transient, we can substitute $\bar{\rho} \approx \rho_0$ into Eq. 58, to obtain

$$\frac{dC}{dt} = k_f h^{-1}(C - C_+(\rho_0))(C - C_-(\rho_0)), \tag{61}$$

where

$$C_\pm(\rho_0) = \frac{1}{2}[(\gamma\rho_0 + h(E_0 + K_M))$$

$$\pm \sqrt{(\gamma\rho_0 + h(E_0 + K_M))^2 - 4hE_0\gamma\rho_0}]. \tag{62}$$

Using the analogy between Eq. 61 and Eq. 51, we can immediately write down the solution to Eq. 61 as

$$C_i(t) = C_-(\rho_0)\left(\frac{1 - e^{-t/t_c}}{1 - (C_-(\rho_0)/C_+(\rho_0))e^{-t/t_c}}\right), \tag{63}$$

where

$$t_C \equiv \frac{1}{k_f h^{-1}(C_+(\rho_0) - C_-(\rho_0))}$$

$$= \frac{h}{k_f \sqrt{(\gamma\rho_0 + h(E_0 + K_M))^2 - 4hE_0\gamma\rho_0}}. \quad (64)$$

The validity of the initial transient depends on its self-consistency (Lin and Segel, 1974). Namely, result 63 is valid for times $t$ such that substitution of $C_i(t)$ into Eq. 45 yields $\bar{\rho} \approx \rho_0$. This criterion can be made explicit by requiring that the fractional decrease of $\bar{\rho}(t)$ during the initial transient should be small (Segel, 1988),

$$\left(\frac{\rho_0 - \bar{\rho}(t)}{\rho_0}\right)t \approx \left(\frac{k_{cat}C}{\rho_0}\right)t \ll 1. \quad (65)$$

Because the duration of the initial transient is on the order of $t_C$ and the maximal value of $C_i(t)$ is $C_-(\rho_0)$, a sufficient condition for the validity of the initial transient, $C_i(t)$, is that

$$\varepsilon \equiv \left(\frac{k_{cat}C_-(\rho_0)}{\rho_0}\right)t_C \ll 1. \quad (66)$$

Assuming that the latter criterion is met, we note that Eq. 63 implies that $C_i(t)$ grows, and, in a time of order $t_C$, approaches the maximal asymptotic value implied by the initial conditions, $C_-(\rho_0)$, which, in turn, implies that the enzyme–substrate complex eventually enters a quasi-steady state such that

$$\frac{dC}{dt} \approx 0, \quad t \geq t_C \quad (67)$$

and

$$C \approx C_-(\bar{\rho}), \quad t \geq t_C. \quad (68)$$

Thus, $\varepsilon \ll 1$ implies the uniformly valid approximation,

$$C(t) = C_-(\bar{\rho})\left(\frac{1 - e^{-t/t_c}}{1 - (C_-(\rho_0)/C_+(\rho_0))e^{-t/t_c}}\right). \quad (69)$$

Moreover, because the validity of Eq. 66 guarantees that the fractional decrease of $\bar{\rho}$ is negligible during the initial transient, the total QSSA (tQSSA) reduces the problem to a single nonlinear rate equation,

$$\frac{d\bar{\rho}}{dt} \approx -k_{cat}C_-(\bar{\rho}), \quad t \geq t_C, \quad (70)$$

subject to the true initial condition

$$\bar{\rho} = \rho_0, \quad t = t_C. \quad (71)$$

In this context, the term total refers to the fact that the QSSA yields an equation for the total undegraded substrate (Borghans et al., 1996). For the tQSSA to hold for all times ($t \geq 0$) the induction period before attainment of quasi-steady state, $t_C$, has to be much shorter than the time scale

for the depletion of $\bar{\rho}$ during the beginning of the tQSS phase (Borghans et al., 1996), $t_{\bar{\rho}}$:

$$\frac{t_C}{t_{\bar{\rho}}} \ll 1. \quad (72)$$

Using result 70, we can estimate

$$t_{\bar{\rho}} \approx \frac{\rho_0}{k_{cat}C_-(\rho_0)} \quad (73)$$

and

$$\frac{t_C}{t_{\bar{\rho}}} = \varepsilon. \quad (74)$$

The latter entails that the validity of Eq. 66 is a sufficient condition for the tQSSA to be uniformly valid for all times. However, because Eq. 70 is nonintegrable, we shall proceed to approximate $C_-(\bar{\rho})$ by a more manageable form, which does allow integration (Borghans et al., 1996).

*The first-order tQSSA*

Defining

$$r(\bar{\rho}) \equiv \frac{4hE_0\kappa\bar{\rho}^{1/2}}{(\kappa\bar{\rho}^{1/2} + h(E_0 + K_M))^2}, \quad (75)$$

we can rewrite Eq. 62 as

$$C_\pm(\bar{\rho}) = \frac{\kappa\bar{\rho}^{1/2} + h(E_0 + K_M)}{2}$$

$$\times (1 \pm \sqrt{1 - r(\bar{\rho})}). \quad (76)$$

The overall behavior of $r(\bar{\rho})$ is determined by the value of the auxiliary parameter

$$\alpha(\bar{\rho}) \equiv \frac{h^{-1}\kappa\bar{\rho}^{1/2}}{E_0 + K_M}. \quad (77)$$

Namely,

$$r(\bar{\rho}) \approx \frac{4E_0\alpha}{E_0 + K_M} \ll 1, \quad \alpha < 1, \quad (78)$$

$$r(\bar{\rho}) \approx r_{max} \equiv \frac{E_0}{E_0 + K_M} < 1, \quad \alpha \approx 1, \quad (79)$$

$$r(\bar{\rho}) \approx \frac{4hE_0}{\kappa\bar{\rho}^{1/2}} < \frac{4}{\alpha} \ll 1, \quad \alpha \gg 1. \quad (80)$$

Note that Eq. 79 entails that

$$r(\bar{\rho}) \approx 1 \Rightarrow h^{-1}\kappa\bar{\rho}^{1/2} \approx E_0 \gg K_M. \quad (81)$$

Hence, unless the enzyme and substrate concentrations are both high, we expect $r$ to be sufficiently small to justify the

expansion of the right-hand side of Eq. 76 to first order in. Such a procedure yields, respectively,

$$C_-(\bar{\rho}) = \frac{\kappa\bar{\rho}^{1/2} + h(E_0 + K_M)}{2} \frac{r}{2}$$

$$= \frac{E_0\kappa\bar{\rho}^{1/2}}{E_0 + K_M + h^{-1}\kappa\bar{\rho}^{1/2}}, \quad r \ll 1, \quad (82)$$

$$C_+(\bar{\rho}) = \kappa\bar{\rho}^{1/2} + h(E_0 + K_M), \quad r \ll 1. \quad (83)$$

Substituting Eqs. 82–83 into Eq. 64, we obtain

$$t_C = \frac{1}{k_f(E_0 + K_M + h^{-1}\gamma\rho_0)}, \quad r \ll 1. \quad (84)$$

and the criterion for the validity of the tQSSA, Eq. 66, reduces to

$$\varepsilon = \frac{\gamma k_{cat}E_0}{k_f(E_0 + K_M + h^{-1}\gamma\rho_0)^2} \ll 1. \quad (85)$$

The latter result can be rewritten in the more revealing form,

$$\left(1 + \frac{K_M + h^{-1}\gamma\rho_0}{E_0}\right) \times \left(1 + \frac{k_r}{k_{cat}} + \frac{E_0 + h^{-1}\gamma\rho_0}{k_{cat}/k_f}\right) \gg \gamma. \quad (86)$$

Because the left-hand side of Eq. 86 is always greater than unity and $\gamma < 1$, we expect Eq. 86 (Eq. 85) to always be at least roughly valid. Moreover, Eq. 86 implies several different conditions, any one of which guarantees that Eq. 85 holds. These are:

$$k_{cat} \ll k_r \Rightarrow K_M \approx K_D, \quad (87)$$

$$K_M + h^{-1}\gamma\rho_0 \gg E_0, \quad (88)$$

$$E_0 \gg \frac{k_{cat}}{k_f}, \quad (89)$$

$$h^{-1}\gamma\rho_0 \gg \frac{k_{cat}}{k_f}. \quad (90)$$

To these we can add the condition

$$h^{-1}\gamma\rho_0 + E_0 \ll K_M, \quad (91)$$

which is directly implied by Eq. 85. Eq. 87 has to be augmented by the requirement that either $\alpha \ll 1$ (low substrate concentration) or $\alpha \gg 1$ (high substrate concentration) to ensure that $r \ll 1$. In contrast, Eqs. 88–91 are sufficient conditions for the validity of the first-order tQSSA because they also guarantee $r \ll 1$. We therefore see that the first-order tQSSA is valid for a wide range of experimental conditions.

Assuming that the first-order tQSSA is valid and substituting Eq. 82 into Eq. 70, we obtain the first-order tQSSA

$$\frac{d\bar{\rho}}{dt} = -\frac{a_2\bar{\rho}^{1/2}}{a_3 + a_1\bar{\rho}^{1/2}}, \quad (92)$$

$$\bar{\rho} = \rho_0, \quad t = 0, \quad (93)$$

where

$$a_1 = h^{-1}\kappa, \quad a_2 = k_{cat}E_0\kappa, \quad a_3 = E_0 + K_M. \quad (94)$$

The solution of this separable initial value problem is found by performing the integral

$$\int \left(\frac{a_1}{a_3} + \frac{a_3}{a_2\bar{\rho}^{1/2}}\right)d\bar{\rho} = \frac{a_1}{a_3}\bar{\rho} + \frac{2a_3}{a_2}\bar{\rho}^{1/2}. \quad (95)$$

Equating this to the integral over $t$ and imposing initial condition 93, we obtain the implicit relation,

$$\frac{a_1}{a_3}\bar{\rho} + \frac{2a_3}{a_2}\bar{\rho}^{1/2} = \frac{a_1}{a_3}\rho_0 + \frac{2a_3}{a_2}\rho_0^{1/2} - t. \quad (96)$$

To solve for $\bar{\rho}$, we recast Eq. 96 into the form of a quadratic equation,

$$a_1z^2 + 2a_3z - a_4 = 0, \quad (97)$$

where

$$z = \bar{\rho}^{1/2}, \quad a_4 = a_1\rho_0 + 2a_3\rho_0^{1/2} - a_2t. \quad (98)$$

Note that $a_4 \geq 0$, because the left-hand side of Eq. 96 is nonnegative, so that both roots of Eq. 97 are real. However, we are only interested in the positive root of Eq. 97,

$$\bar{\rho}^{1/2} = z_+ \equiv \frac{\sqrt{a_3^2 + a_1a_4} - a_3}{a_1}. \quad (99)$$

Finally, whenever $\varepsilon \ll 1$ and $r \ll 1$, the first-order tQSSA is valid, and Eqs. 82 and 83 imply

$$\frac{C_-(\rho_0)}{C_+(\rho_0)} \approx \frac{r(\rho_0)}{4} \quad (100)$$

Incorporating Eqs. 100 and 82 into Eq. 69 yields

$$C = C_-(\bar{\rho})\left(\frac{1 - e^{-t/t_C}}{1 - (r/4)e^{-t/t_C}}\right)$$

$$\approx \frac{E_0\kappa\bar{\rho}^{1/2}(1 - e^{-t/t_C})}{E_0 + K_M + h^{-1}\kappa\bar{\rho}^{1/2}}, \quad (101)$$

where $t_C$ and $\bar{\rho}$ are given by Eqs. 84 and 99, respectively.

Although results 99 and 101 formally solve the problem, they involve many parameters and are not very illuminating. We shall therefore pause to derive analytical approximations for some important limiting cases of the first-order tQSSA, which are guaranteed to be valid by Eqs. 89–91.

*Important limiting cases*

At sufficiently high enzyme concentrations, such that $E_0 \gg \max(h^{-1}\gamma\rho_0, K_M)$, Eqs. 82 and 92 reduce to, respectively,

$$C_-(\bar{\rho}) \approx \kappa\bar{\rho}^{1/2}, \tag{102}$$

$$\frac{d\bar{\rho}}{dt} \approx -k_{cat}\kappa\bar{\rho}^{1/2}. \tag{103}$$

Solving the latter equation yields the approximations

$$\frac{\bar{\rho}}{\rho_0} \approx \left(1 - \frac{\gamma k_{cat}}{2} t\right)^2, \tag{104}$$

$$C \approx \gamma\rho_0\left(1 - \frac{\gamma k_{cat}}{2} t\right)(1 - e^{-k_f E_0 t}). \tag{105}$$

The validity of these results is guaranteed by Eq. 89.

The case of low enzyme concentration, $E_0 \ll K_M$, has to be dealt with in more detail. If $E_0 \ll K_M$ and the monomer concentration is high, $h^{-1}\gamma\rho_0 \gg K_M$, then Eq. 90 holds and Eqs. 82 and 92 reduce, respectively, to

$$C_-(\bar{\rho}) \approx hE_0, \tag{106}$$

$$\frac{d\bar{\rho}}{dt} \approx -hk_{cat}E_0, \tag{107}$$

so that

$$\bar{\rho} \approx \rho_0 - hk_{cat}E_0 t, \tag{108}$$

$$C \approx hE_0(1 - e^{-k_f h^{-1}\gamma\rho_0 t}). \tag{109}$$

Otherwise, if the enzyme and monomer concentrations are both low, then Eq. 91 holds and Eqs. 82 and 92 reduce to, respectively,

$$C_-(\bar{\rho}) \approx \frac{\kappa E_0}{K_M} \bar{\rho}^{1/2}, \tag{110}$$

$$\frac{d\bar{\rho}}{dt} \approx -\frac{k_{cat}\kappa E_0}{K_M} \bar{\rho}^{1/2}, \tag{111}$$

so that

$$\frac{\bar{\rho}}{\rho_0} \approx \left(1 - \frac{t}{T_{max}}\right)^2, \quad T_{max} = \frac{2K_M}{\gamma k_{cat}E_0}, \tag{112}$$

$$C \approx \frac{\gamma\rho_0 E_0}{K_M}\left(1 - \frac{t}{T_{max}}\right)(1 - e^{-(k_{cat}+k_r)t}). \tag{113}$$

Two general conclusions emerge from this analysis. First, that the dependence of the rate of erosion, $d\bar{\rho}/dt$, upon the initial enzyme concentration is governed by an apparent Michaelis–Menten constant, $K_{M, app}$, defined as

$$K_{M, app} \equiv K_M + h^{-1}\gamma\rho_0. \tag{114}$$

Namely, the erosion rate is proportional to the initial enzyme concentration if $E_0 \ll K_{M, app}$, and is practically independent of the initial enzyme concentration if $E_0 \gg K_{M, app}$. Second, Eqs. 104 and 112 both predict a linear decrease of the square root of the substrate concentration with time, which is consistent with ideal surface erosion of the fibrils (Hayashi and Ikada, 1990). Moreover, the condition $h^{-1}\gamma\rho_0 \ll K_M$ is also satisfied in the case of a single thick fibril immersed in an excess of enzyme solution, such that $\gamma \ll 1$, and $h \gg 1$. Namely, the tQSSA prediction of the proposed model provides a definitive prediction for the rate constant appearing in the phenomenological surface erosion model proposed by Hayashi and Ikada (1990) for the enzymatic erosion of insoluble fibers.

## PARAMETER ESTIMATION SCHEME

The general reaction diffusion model depends on twelve model parameters: four diffusivities, two length scales, one for the fibrillar matrix and the other for the solution layer, the initial enzyme and monomer concentrations $E_0$ and $\rho_0$, one structural parameter $\gamma$, and three independent kinetic parameters $k_f$, $k_r$, and $k_{cat}$. Because the initial concentrations and the length scales are controllable quantities, in general, only eight parameters have to be estimated to simulate a given experiment (which is less than the number of independent dimensionless variables for this problem). When the limit of instantaneous diffusion is valid, only four model parameter values have to be estimated, because the diffusivities are effectively infinite. This is relevant for thin sparse gels in well-mixed enzymatic solutions.

In this section, we shall demonstrate how it is possible to sequentially estimate all four parameters of the limit of instantaneous diffusion by combining direct optical methods and equilibrium binding experiments, which are of general validity, with transient erosion experiments for which the first-order tQSSA is guaranteed to be valid by either of criteria 89–91.

### Step 1: estimating $\gamma$ and $K_D$

According to its definition in Eq. 20, $\gamma$ is proportional to the ratio of the diameter of a monomer in the fibril, $d_m$, and the initial diameter of the fibril, $d_f(0)$. The former is a known quantity and the latter can be estimated using standard optical methods (Kadler et al., 1996), thereby allowing a direct estimate of $\gamma$ (Welgus et al., 1980). As we will show in a moment, $\gamma$ can also be estimated by analyzing equilibrium binding data. It is crucial for the validity of Eq. 17 that both methods of estimating $\gamma$ yield consistent results.

Equilibrium binding experiments may be fitted to

$$C_{eq} = \tfrac{1}{2}\left[(\gamma\rho_0 + h(E_0 + K_D))\right.$$

$$\left. - \sqrt{(\gamma\rho_0 + h(E_0 + K_D))^2 - 4hE_0\gamma\rho_0}\right], \quad (57)$$

to estimate $\gamma$ and $K_D$. The limits

$$\lim_{E_0\to\infty} C_{eq} = \gamma\rho_0, \quad (115)$$

$$\lim_{E_0\to 0} C_{eq} = \frac{\gamma\rho_0}{K_D + h^{-1}\gamma\rho_0}, \quad (116)$$

imply that such a fit is unambiguous because $\gamma$ is determined by the limit of high enzyme concentration, whereas $K_D$ is determined by the opposite limit. Alternatively, $\gamma$ and $K_D$ can be estimated by fitting the equilibrium binding results to the prediction implied by Eq. 22

$$C_{eq} = \frac{\gamma\rho_0 E_{eq}}{K_D + E_{eq}}, \quad (117)$$

where $E_{eq}$ is the concentration of free enzyme at equilibrium. Both Eqs. 57 and 117 are exact predictions of the low-temperature limit of the model equations (Eqs. 34–39).

## Step 2: estimating $k_{cat}$ and $K_M$

First, Eq. 104 can be used to estimate $k_{cat}$ from transient erosion experiments at high enzyme concentrations, $E_0 \gg K_D + h^{-1}\gamma\rho_0$. Subsequently, Eq. 112 can be used to estimate the ratio $k_{cat}/K_M$ from transient erosion experiments at low enzyme and substrate concentrations, such that $E_0 + h^{-1}\gamma\rho_0 \ll K_D$. Instead of actually using a matrix with a lower substrate concentration, $\rho_0$, the value of $h^{-1}\gamma\rho_0$ can be made negligible by decreasing $h^{-1}$ sufficiently. The latter is attained by increasing the ratio of the volume of the enzyme solution to the volume of the matrix, and using vigorous mixing to ensure the validity of the limit of instantaneous diffusion.

For completeness, and also to allow comparison with the literature, we shall consider the alternative of using a double reciprocal plot for estimating $K_M$ and $\gamma k_{cat}$. However, as will become evident, the latter approach is inferior to the sequential approach advocated above.

Assuming that the tQSSA is valid, Eq. 72 implies that we can find $\Delta t$ such that

$$t_C \ll \Delta t \ll t_{\bar{\rho}} \quad (118)$$

and

$$P(\Delta t) \approx P(t_C) + (\Delta t - t_C)\left.\frac{dP}{dt}\right|_{t_C}$$

$$\approx -\Delta t\left.\frac{d\bar{\rho}}{dt}\right|_{t_C} \approx -\Delta t k_{cat}C_-(\bar{\rho}(t_C)). \quad (119)$$

Substituting Eq. 82 into Eq. 119 and using the estimate $\kappa\bar{\rho}^{1/2}(t_C) \approx \gamma\rho_0$, we find

$$\frac{P(\Delta t)}{\Delta t} \approx -k_{cat}C_-(\bar{\rho}(t_C)) \approx \frac{\gamma k_{cat}E_0\rho_0}{E_0 + K_M + h^{-1}\gamma\rho_0}. \quad (120)$$

The latter result can be rearranged as

$$\frac{\rho_0\Delta t}{P(\Delta t)} \approx \frac{E_0 + K_M + h^{-1}\gamma\rho_0}{\gamma k_{cat}E_0\rho_0}$$

$$= \frac{1}{\gamma k_{cat}} + \left(\frac{K_M + h^{-1}\gamma\rho_0}{\gamma k_{cat}}\right)\frac{1}{E_0}. \quad (121)$$

Namely, as in the case of enzymatic reactions in solution, provided that the first-order tQSSA is valid, a double reciprocal plot of $(\rho_0\Delta t)/P(\Delta t)$ versus $1/E_0$ should yield a straight line, and allow us to estimate $k_{cat}$ from its intercept and $K_M$ from its slope. The validity of the first-order tQSSA can be guaranteed a priori by conducting the experiments at very low or very high enzyme concentrations. The principle disadvantage of the double reciprocal plot is that it is difficult to take a sufficient number of measurements subject to Eq. 118.

## Step 3: estimating $k_f$ and $k_r$

The definition of $K_M$, Eq. 50, implies the following lower bound for $k_f$,

$$k_f \geq \frac{k_{cat}}{K_M} \equiv \left(\frac{k_{cat}}{k_{cat} + k_r}\right)k_f. \quad (122)$$

Hence, the estimates of $K_M$ and $k_{cat}$ obtained in Step 2 can be used to obtain a lower bound estimate of $k_f$. This initial estimate can be improved by conducting an erosion experiment subject to Eq. 89 (Eq. 90) and fitting the concentration of bound enzyme to Eq. 105 (Eq. 109) to obtain $k_f$ and $k_r \equiv k_f K_M - k_{cat}$. Alternatively, the erosion experiment can be conducted subject to Eq. 91, and $k_r$ and $k_f \equiv (k_r + k_{cat})/K_M$ can be estimated by fitting the concentration of bound enzyme to Eq. 113. From a practical point of view, it may be simpler to measure the concentration of free enzyme in the solution and to use the global enzyme conservation result, $C = h(E_0 - E)$, than to directly measure the concentration of bound enzyme in the gel. The idea of estimating $k_f$ by fitting a uniformly valid approximation of $C$ to experimental results at high enzyme concentrations has re-

cently been proposed by Schnell and Maini (2000) for enzymatic reactions in solution.

## COMPARISON TO EXPERIMENT

An ideal problem for testing the proposed model and parameter estimation method is the degradation of fibrillar collagen by skin fibroblast collagenase. The latter is a highly specific enzyme that dissolves fibrils of type I, II, and III interstitial collagens by making a single scission across all three $\alpha$ chains of exposed triple-helical collagen monomers at a specific collagen locus that has been identified (Welgus et al., 1981; Wu et al., 1990). This hyperactive site is located approximately three-quarters from the N-terminus of the collagen monomer to yield the so-called $TC^A$ and $TC^B$ fragments. Despite the solid nature of the fibrillar collagen substrate, the site of specific collagenase cleavage appears to be the same as for collagen monomers in solution (Welgus et al., 1980). At temperatures below 34°C, these initial fragments maintain their triple helical structure and are resistant to further proteolytic attack. However, at 37°C the two products of collagenase cleavage spontaneously denature into nonhelical gelatin derivatives (Sakai and Gross, 1967; Bleeg, 1991). With the loss of the triple-helical structure, these peptides become susceptible to further degradation by gelatinases A and B, and, to a lesser degree, by fibroblast collagenase (Welgus et al., 1982). Moreover, the kinetics of the initial cleavage of native and denatured monomeric collagen in solution is well described by Michaelis–Menten kinetics (Welgus et al., 1981a; Welgus et al., 1982; Hasty et al., 1987; Mallya et al., 1992). Whereas the value of $K_M$ is on the order of 1 $\mu$M almost independent of enzyme and collagen type, the variability in $k_{cat}$ is high (Welgus et al., 1982; Hasty et al., 1987). Such low values of $K_M$ are a manifestation of the strong binding of collagenase to native and denatured collagen monomers, and are consistent with the observation of very low concentrations of free collagenase in vivo (Lapiere and Gross, 1963).

For definiteness we shall consider the experiments of Welgus et al. (1980) on the erosion of sparse fibrillar collagen gels by skin fibroblast collagenase. These authors carried out a comprehensive study of enzyme binding and gel erosion as a function of temperature, enzyme concentration, gel weight, and the volume of enzyme solution. Moreover, they used the methods of Step 1 to estimate $\gamma$ and $K_D$ at 25°C, and a prebinding-temperature jump experiment to estimate $k_{cat}$, but they were unable to estimate $K_M$ in lieu of an appropriate kinetic model. In this section, we shall use the estimates of $\gamma$ and $k_{cat}$ obtained by Welgus et al. (1980) to obtain an estimate of $K_M$ by fitting our model equations to a specific transient erosion experiment reported by these authors. We will then use our estimate of $K_M$ along with the reported estimates of $\gamma$ and $k_{cat}$ to simulate additional experiments by these authors. This will serve the double purpose of elucidating the role of diffusion in these experiments and partially validating the estimate of $K_M$.

## Numerical methods

Eqs. 22–33 are highly nonlinear and stiff and were therefore solved numerically using the finite element program FIDAP (1993). The finite element method (FEM) is a general method used for numerical solution of partial differential equations (Hughes, 1987). The interested reader can find a concise account of the FEM formulation for reaction diffusion problems in diffusion in (Aharon et al., 1996; Tzafriri, 2000). In the present paper, the geometry of the matrix and the adjacent solution layer was modeled as a two-dimensional rectangular mesh using linear four-node quadrilateral elements (interpolation functions). The use of symmetry boundary conditions (e.g., zero flux) allowed us to model only a quarter of the physical geometry. The heterogeneity of the problem suggested that we use a nonuniform mesh with twice as many elements in the matrix as in the solution layer, and a smooth transition in the region of the gel–liquid interface. The absence of a boundary condition at the gel–liquid interface is equivalent to an imposition of flux continuity in the FEM (Hughes, 1987). The resulting algebraic equations were integrated using the backward Euler method with variable time stepping and up to ten inner quasi-Newton iterations (FIDAP, 1993). The results discussed below were all obtained using 600 elements (e.g., 400 elements for the matrix and 200 for the solution layer), because this was shown to ensure convergence. Namely, further refinement of the mesh did not significantly affect the results.

The kinetic equations corresponding to the limit of instantaneous diffusion, Eqs. 45–48, were solved numerically using a stiff integrator ODE23s provided in MATLAB 5.3 (Shampine and Reichlet, 1997). Data analysis was performed using GraphPad Prism 3.02. The Levenberg–Marquardt method (Marquardt, 1963) was used to minimize the unweighted sum of squares of the difference between the experimental data and the theoretical data generated by one of the closed-form solutions of the model equations in the limit of instantaneous diffusion (see The limit of instantaneous diffusion).

## Preliminary estimates

The concentration of the fibrillar collagen gels used by Welgus et al. (1980) was 4 mg/ml in all the experiments. Using an average molecular mass of 300 kDa for a single collagen monomer (triple-helix), we find $\rho_0 = 13.3$ $\mu$M, which corresponds to an initial volume fraction, $\phi_0$, of 0.003. Because 99.7% of the mesh is taken up by the fluid, the diffusion coefficients of the free enzyme and the degradation products in the gel are expected to be near their value in water (Ogston et al., 1976; Weadock et al., 1987;

Gilbert et al., 1988; Saltzman et al., 1994). For simplicity, we assume that all the diffusivities are equal to the diffusion coefficient of bovine serum albumin (BSA) at body temperature (Peppas and Reinhart, 1984),

$$D_{e,g} = D_{e,s} = D_{p,g} = D_{p,s} = 7.4 \times 10^{-7} \text{ cm}^2/\text{s}. \quad (123)$$

This assumption is plausible because all these molecules have approximately the same molecular mass and Stokes radii (Tyn and Gusek, 1990). Namely, the molecular mass of skin fibroblast collagenase and BSA are 60 kDa and 66 kDa, respectively, and the average molecular mass of the uncoiled cleavage products is approximately 50 kDa (three fragments with a molecular mass of approximately 25 kDa and three larger fragments with an approximate molecular mass of 75 kDa).

Direct spectroscopic measurement of the collagen fibrils yielded the estimate $0.06 \leq \gamma \leq 0.12$ (50 nm $\leq d_f(0) \leq 100$ nm) (Welgus et al., 1980). At 25°C, the measured erosion rate drops to less than 5% of the value measured at 37°C. Welgus et al. (1980) utilized this observation to measure the equilibrium binding curves of the enzyme at 25°C and used Eq. 117 to estimate $\gamma = 0.09$ and $K_D = 0.95$ μM. The rate of catalysis at 37°C, $k_{cat}$, was estimated by prebinding the enzyme at 25°C, determining the amount of bound enzyme by supernatant analysis and then transferring the gel into a second test tube with the same buffer (but free of enzyme) at 37°C and counting the number of collagen molecules degraded per collagenase molecule per hour. Because the degradation kinetics are linear in time, this turnover number may be used to estimate $k_{cat}$. In this way, these authors found $k_{cat} = 25 \text{ h}^{-1}$, regardless of the enzyme concentration of the prebinding solution (Welgus et al., 1980). This estimate will be re-examined after we estimate $K_M$.

Finally, because the heterogeneous nature of this problem was not fully appreciated by these authors, the thickness of the fibrillar gel samples was not reported. However, this value may be estimated indirectly by fitting the experimental release of the zymogen (inactive enzyme) from the fibrillar gel. Welgus et al. (1980) found that 30% of the zymogen was released from a 200-μg gel sample within 1 min, and equilibrium was achieved 15 min post immersion. Assuming a slab geometry for the gel, we find

$$L \approx \sqrt{D_{e,g} \times 900} = 0.026 \text{ cm}.$$

Trial-and-error fitting of the numerical simulation to the experimental results of Welgus et al. (1980) for the 200-μg slab yielded

$$L \approx 0.02 \text{ cm} = 200 \text{ μm}. \quad (124)$$

## Estimation of $K_M$

Table 1 shows parameter estimates corresponding to the erosion experiments of Welgus et al. (1980). Because the time scale for the diffusion of enzyme into this sample,

**TABLE 1 Initial conditions and preliminary parameter estimates**

| $k_{cat}$ (h$^{-1}$) | $K_D$ (μM) | $\gamma$ | $D_{e,g}$ (cm$^2$/s) | $h$ | $L$ (μm) | $\rho_0$ (μM) | $E_0$ (μM) |
|---|---|---|---|---|---|---|---|
| 25 | 0.95 | 0.09 | $7.4 \times 10^{-7}$ | 4 | 100 | 13.3 | 0.26 |

Parameter estimates for the transient erosion experiment of Welgus et al. (1980). The value of $k_{cat}$ corresponds to the turnover rate at 37°C. The value of $K_D$ was estimated at 25°C. $\gamma$ is estimated directly from Eq. 20, with $d_m = 1.5$ nm (Hulmes et al., 1995) and the average value $d_f = 75$ nm as obtained by scanning electron microscopy (Welgus et al., 1980). $D_{e,g}$ is estimated using the experimental diffusion coefficient of BSA in water (Peppas and Reinhart, 1984).

$L^2/D_{e,g} = 2.3$ min, is short compared to the duration of the experiment (90 min), the limit of instantaneous diffusion is likely to be at least roughly valid for this experiment. Moreover, the a priori estimate $K_M(37°C) \approx K_D(25°C) \approx 1$ μM implies $\varepsilon \approx 0.01$ and $r(\rho_0) \approx 0.12$. Hence, it is plausible to assume that the exact tQSSA is valid and that the first-order tQSSA is at least roughly valid for this experiment. Both these conclusions are important. The first because it implies that the experimental erosion kinetics depend only on the tQSSA kinetic parameters, $\gamma$, $k_{cat}$, and $K_M$, and the latter because it implies that we may use some of our analytical results to estimate $K_M$. Unfortunately, the estimates $E_0 \approx h^{-1}\gamma\rho_0$ and $E_0 + h^{-1}\gamma\rho_0 = 0.55$ μM implied by Table 1 entail that approximate analytical results corresponding to the limits of high or low enzyme concentration are invalid for this experiment, which means that Step 2 of the proposed parameter estimation method cannot be used to evaluate $K_M$. Moreover, the self-consistency of neglecting diffusion in estimating $K_M$ has to be validated. We therefore estimated $K_M$ by sequentially fitting the experimental results first to the first-order tQSSA result, Eq. 99, then to the numerical solution of the kinetic equations corresponding to the limit of instantaneous diffusion, Eqs. 45–48, and finally to the numerical solution of the full reaction diffusion model, Eqs. 22–33. This approach relies heavily on the fact that, although the validity of the first-order tQSSA may be marginal for this experiment, the exact tQSSA is expected (and verified) to be valid, which means that the initial transient can safely be neglected and that the specific values of $k_f$ and $k_r$ are unimportant, provided that $K_M = (k_r + k_{cat})/k_f$. For simplicity, we use the values $k_r = 0$ and $k_f = k_{cat}/K_M$ in all subsequent numerical simulations.

Using nonlinear regression to fit the experimental results to the first-order tQSSA result, Eq. 99, with $K_M(37°C) \approx K_D(25°C) \approx 1$ μM (see Table 1) as an initial guess yielded the estimate $K_M \approx (0.36 \pm 0.02)$ μM ($r^2 = 0.99$). Seemingly, this is a very good estimate with a low standard error (7%). However, as can be seen in Fig. 4, the approximate analytical result begins to deviate from the numerical solution of kinetic Eqs. 45–48 at $t = 0.5$ h. This observation is consistent with the fact that $r(\rho_0) \approx 0.37$ and $\varepsilon \approx 0.01$ for these simulations, which implies that the exact tQSSA is
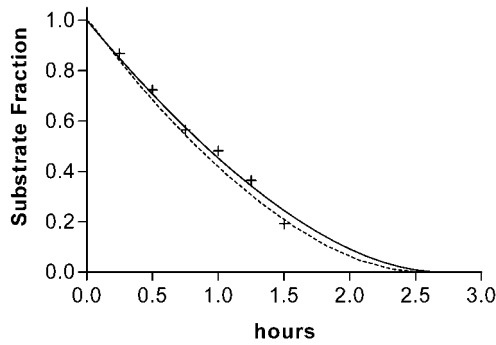
FIGURE 4 Preliminary estimate of $K_M$ using the tQSSA. (+) Experimental results for a 100-$\mu$g gel sample incubated at 37°C with 75 $\mu$l enzyme solution with a postmixing enzyme concentration of 0.26 $\mu$M (adapted from Fig. 1 $C$ in Welgus et al., 1980). *Solid line*, Evaluation of Eq. 99 with parameter values from Table 1 and $K_M = 0.36$ $\mu$M. *Dashed line*, Numerical solution of kinetic Eqs. 45–48 using the parameter values shown in Table 1, $K_M = 0.36$ $\mu$M, $k_r = 0$ and $k_f = k_{cat}/K_M$.



FIGURE 5 Refined estimate of $K_M$ using the full reaction diffusion model. (+) Experimental results for a 100-$\mu$g gel sample incubated at 37°C with 75 $\mu$l enzyme solution with a postmixing enzyme concentration of 0.26 $\mu$M (adapted from Fig. 1 $C$ in Welgus et al., 1980). *Dashed line*, Numerical solution of kinetic Eqs. 45–48 with parameter values from Tables 1 and 2. *Solid line*, Reaction diffusion simulation with parameter values from Tables 1 and 2.

valid but that the first-order tQSSA is only roughly valid. Trial-and-error numerical solution of Eqs. 45–48 yielded the slightly higher estimate $K_M \approx 0.45$ $\mu$M. Once more, the exact tQSSA is found to be valid for these simulations, $\varepsilon \approx 0.01$, whereas the first-order tQSSA is only of marginal validity, $r(\rho_0) \approx 0.30$. Note that the latter fit implies $K_M \approx K_D$ so that $k_{cat} \ll k_r$ and $k_f \gg k_{cat}/K_M \approx 5.6 \times 10^7$ $M^{-1}h^{-1}$.

The above estimate of $K_M$ was obtained under the assumption that the limit of instantaneous diffusion is valid. To determine how the estimate of $K_M$ is affected by the introduction of diffusion into the analysis, the reaction diffusion model was simulated using the parameter values shown in Tables 1 and 2. As can be seen in Fig. 5, the reaction diffusion simulation predicts a slightly lower rate of erosion compared to the corresponding kinetic simulation. This is not surprising because the time scale for diffusion, $L^2/D_{e,g} = 2.3$ min, is short compared to the initial time scale for degradation, $t_{\bar{\rho}} \approx 20$ min, but is slightly longer than the estimated duration of enzyme adsorption, $t_C \approx 1.1$ min.

## Reexamination of the estimate of $k_{cat}$

We now reexamine the validity of the experimental estimate of $k_{cat}$ obtained by Welgus et al. (1980). In a typical experiment reported by these authors, 200 $\mu$g (50 $\mu$l) of fibrillar

collagen were equilibrated at 25°C for 20 min with 50 $\mu$l of a buffer solution that contained 1.56 $\mu$g enzyme and then transferred to a buffer at 37°C to estimate the average turnover rate. Substituting the values corresponding to such an experiment ($E_0 = 0.27$ $\mu$M, $h = 2$, $\gamma = 0.09$ and $K_D = 0.95$ $\mu$M) into Eq. 57, we obtain $C_{eq} = 0.18$ $\mu$M. Figure 6 shows the fractional erosion obtained from the numerical solution of Eqs. 45–47 with the initial conditions $C(0) = 0.18$ $\mu$M and the parameter values shown in Tables 1 and 2. As can be seen, the fraction of undegraded collagen monomers decreases linearly with time in the first hour of degradation. Fitting these results to the initial asymptote implied by Eq. 25,

$$\frac{\bar{\rho}}{\rho_0} = 1 - k_{cat}C(0)t, \qquad (125)$$



FIGURE 6 Fraction of undegraded collagen monomers at 37°C after preincubation at 25°C. (+) Numerical solution of kinetic Eqs. 45–48 with the initial conditions $C(0) = 0.18$ $\mu$M and the parameter values shown in Tables 1 and 2. *Solid line*, Linear regression of the simulation results according to Eq. 125. See text for details.

**TABLE 2 Fitted kinetic parameter values**

| $K_M$ ($\mu$M) | $k_r$ | $k_f$ ($M^{-1}$ $h^{-1}$) |
| --- | --- | --- |
| 0.45 | 0 | $5.6 \times 10^7$ |

Kinetic parameter values obtained by fitting the reaction diffusion model to the transient degradation results of Welgus et al. (1980). See text for details.
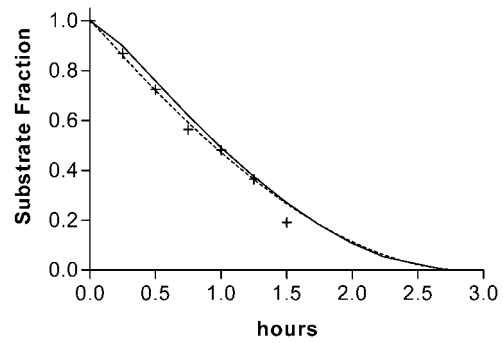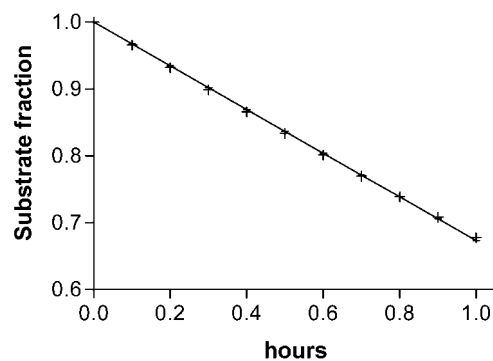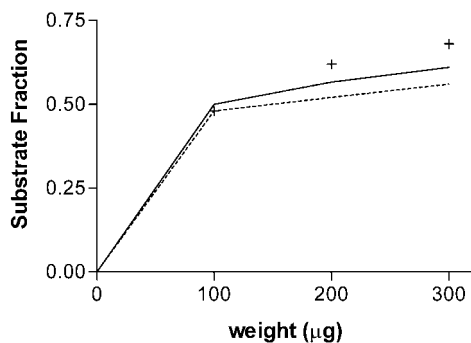
FIGURE 7 Erosion rate versus matrix weight/thickness. (+) Experimental results (adapted from Fig. 1 *D* in Welgus et al., 1980). *Solid line*, Reaction diffusion simulation. *Dashed line*, Numerical simulation of kinetic Eqs. 45–48. See text for more details.

yielded the estimate $k_{cat} = (34.4 \pm 0.17)$ h$^{-1}$. The prebinding method used by Welgus et al. (1980) to estimate $k_{cat}$ can therefore lead to a 50% error. The source of this error lies in the fact that $K_D = 0.95$ $\mu$M was used to calculate $C_{eq}$ for the prebinding at 25°C, whereas, after the temperature jump, $K_D \approx K_M = 0.45$ $\mu$M was used in the numerical simulation of Eqs. 45–47. This argument was verified by repeating the above analysis with the sole modification of using $K_D = K_M = 0.95$ $\mu$M in the numerical simulation of Eqs. 45–47. Such a procedure yielded the estimate $k_{cat} = (23.9 \pm 0.10)$ h$^{-1}$, which is almost the same as the value used in the simulation, $k_{cat} = 25.0$ h$^{-1}$.

## Diffusion effects

Diffusion was shown to have a minor effect in the experiments analyzed above. A disparity between the reaction diffusion simulation and the corresponding limit of instantaneous diffusion becomes evident as the diffusion path increases. This is demonstrated in Fig. 7, which compares experimental results for the fraction of undegraded collagen monomers remaining at the end of one hour to the corresponding numerical simulation results. Experimental results correspond to the erosion of gel samples of increasing weight (100–300 $\mu$g) in 75 $\mu$l of a 0.26-$\mu$M solution of collagenase (Welgus et al., 1980). Numerical simulations use the parameter values shown in Tables 1 and 2, except for $L$ and $h$. Increasing the weight of the gel is equivalent to increasing $L$ and a decreasing $h$, and therefore to a decrease in the measured erosion rate with increase in sample weight. As can be seen in Fig. 7, this trend is captured by the reaction diffusion simulation and, to a lesser extent, by the simulation of kinetic Eqs. 45–48, because the latter correspond to the limit $L^2/D_{e,g} \to 0$.

An alternative way of increasing the characteristic time scale for diffusion is by increasing the amount of enzyme solution used in the experiment, because this results in a thicker solution layer. This is considered in Fig. 8, which
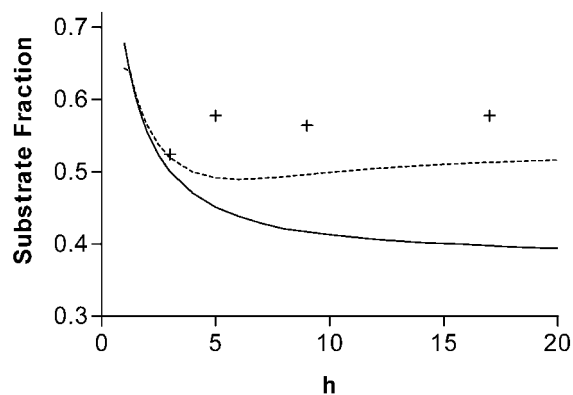


FIGURE 8 Fraction of undegraded collagen molecules after incubation for 1 h with different volumes of enzyme solution (+) Experimental results for a 100-$\mu$g gel sample incubated at 37°C with 75 $\mu$l enzyme solution with a postmixing enzyme concentration of 0.26 $\mu$M (adapted from Fig. 1 *B* in Welgus et al., 1980). *Dashed line*, Reaction diffusion simulations using the model parameter values shown in Tables 1 and 2. *Solid line*, Numerical simulation of kinetic Eqs. 45–48 using the model parameter values shown in Tables 1 and 2.

compares theoretical predictions to experimental results for a 100 $\mu$g gel sample incubated at 37°C for 1 h with 50, 100, 200, and 400 $\mu$l of collagenase solution with a postmixing concentration of 0.26 $\mu$M. The numerical simulations of the reaction diffusion equations and of the kinetic model were conducted using $L = 100$ $\mu$m and the parameter values shown in Tables 1 and 2, except for $h$, which is proportional to the volume of enzyme solution. As can be seen, the reaction diffusion simulation captures the qualitative behavior of experimental results rather well. In contrast, the kinetic model predicts a monotonic decrease of the rate of erosion as the volume of enzyme solution (the value of $h$) is increased, which is consistent with the observation that, as $h^{-1}$ decreases, the denominator on the right-hand side of Eq. 92 increases. The latter is a manifestation of the fact that more enzyme is available for binding at the gel–solution interface. Interestingly, the decrease in the erosion rate as a result of the increase in the diffusion path is more than compensated by the increase associated with the kinetic effects.

## Erosion rate versus enzyme concentration

Using the parameter estimates in Tables 1 and 2, we next consider the dependence of the initial rate of erosion on the enzyme concentration. This is illustrated in Fig. 9, which shows the fraction of undegraded collagen molecules in the gel at the end of 0.1 h (6 min) of incubation. Because there are no quantitative experimental measurements of this kind, we only show numerical simulation results. As can be seen in Fig. 9, the role of diffusion is not very significant at all concentrations and diminishes with enzyme concentration. According to our reaction diffusion simulation, deviation
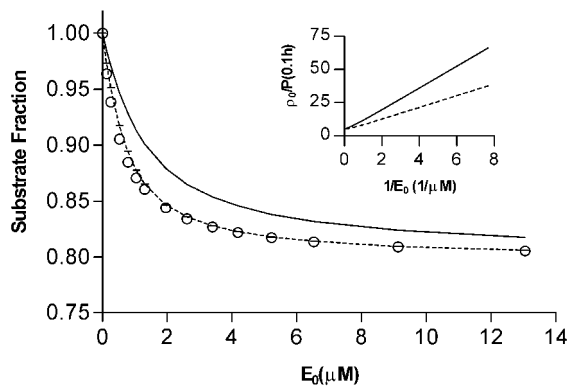
FIGURE 9   Fraction of undegraded collagen molecules at the end of 0.1-h incubation at 37°C, with varying enzyme concentrations. *Solid line*, Reaction diffusion simulations using the model parameter values shown in Tables 1 and 2. *Dashed line*, Numerical simulation of kinetic Eqs. 45–48 using the model parameter values shown in Tables 1 and 2. (○) Evaluation of Eq. 99 using the model parameter values shown in Tables 1 and 2. Insert shows the double-reciprocal plot of the numerically simulated results (see text for details).

from linearity occurs at a threshold concentration of ~1.0 μm. The double-reciprocal plots of the simulations appearing in Fig. 9 are illustrated in the insert to that figure. As can be seen, both plots are indeed linear. Moreover, weighted linear regression yielded the estimates

$$(\gamma k_{cat})^{-1} = (0.47 \pm 0.01) \text{ h}, \qquad (126a)$$

$$\frac{K_M + h^{-1} \gamma \rho_0}{\gamma k_{cat}} = (0.75 \pm 0.15) \ \mu\text{M h}^{-1}, \quad (126b)$$

for the reaction diffusion simulation ($r^2 = 1.0$) and

$$(\gamma k_{cat})^{-1} = (0.47 \pm 0.01) \text{ h}, \qquad (127a)$$

$$\frac{K_M + h^{-1} \gamma \rho_0}{\gamma k_{cat}} = (0.40 \pm 0.01) \ \mu\text{M h}^{-1}, \quad (127b)$$

for the kinetic simulation ($r^2 = 1.0$). Substituting the known values of $h$, $\gamma$, and $\rho_0$ into these results, we find that the double-reciprocal plot yields the average estimates $k_{cat} = 25.0 \text{ h}^{-1}$ ($k_{cat} = 24.8 \text{ h}^{-1}$) and $K_M = 0.58 \ \mu\text{M}$ ($K_M = 1.32 \ \mu\text{M}$) for the kinetic (reaction diffusion) simulation. Thus, the (extrapolated) intercept of the double-reciprocal plot with the horizontal axis yields a good estimate of $\gamma k_{cat}$ ($k_{cat}$) in both cases. In contrast, the estimate of the slope is significantly different for the reaction diffusion simulation and the kinetic simulation and only yields an order of magnitude estimate of $K_M$ in both cases. This is because the largest contribution to the double-reciprocal plot estimate of $K_M$ comes from the range of intermediate enzyme concentrations. Unfortunately, the validity of the double-reciprocal plot depends on the validity of the first-order tQSSA, and the latter may not be valid for intermediate enzyme concentrations. Unless it is ex-

tremely fast, diffusion only increases the ambiguity in the estimated $K_M$, because it delays the establishment of the QSS to times on the order of $L^2/D_{e,g} > t_C$.

We therefore conclude that, even when diffusion effects are present, the double-reciprocal plot can yield a straight line and can be used to estimate $k_{cat}$, but not $K_M$. Namely, linearity of the double-reciprocal plot is not a sufficient criterion for ensuring that it yields a good estimate of $K_M$.

## DISCUSSION

In this work, we derived a reaction diffusion model to describe the enzymatic degradation and erosion of insoluble fibrillar matrices. The novel feature of this model is the derivation of kinetic equations subject to the experimental indications that, due to steric hindrance, the relatively large enzyme molecules cannot penetrate the fibrils, so that the only sites available for enzyme binding are located at the surface of the fibrils (Steven, 1976a,b; Viikari et al., 1991). The enzymatic degradation process was modeled using the standard Michaelis–Menten scheme, which has been shown to apply to the degradation of collagen monomers in solution by mammalian collagenase (Welgus et al., 1981a; Welgus et al., 1982; Hasty et al., 1987). Moreover, a recent real-time imaging study (Lin et al., 1999) found that the proteolysis of surface-adsorbed collagen monomers by purified *Clostridium histolyticum* collagenase is well described by the Michaelis–Menten scheme with $K_M$ and $k_{cat}$ values taken from the corresponding experiments on bulk degradation in solution (Mallya et al., 1992).

In this work, we only consider sparse fibrillar gels such that the initial volume fraction of the fibers in the gel, $\phi_0$, is less than 0.1. This restriction is justified for many artificial gels (Welgus et al., 1980; Gilbert and Kim, 1990; Riesle et al., 1998; Compton et al., 1998; Zhu et al., 2001) and for certain connective tissues (Riesle et al., 1998; Brilla et al., 2000), and allows us to neglect partitioning effects (Ogston, 1958; Fanti and Glandt, 1990a,b) and to use simple estimates for the diffusion coefficients of the enzyme and the degradation products (Ogston et al., 1976; Peppas and Reinhart, 1984; Weadock et al., 1987; Gilbert et al., 1988). Moreover, for sufficiently thin gels, the characteristic timescale of diffusion is comparable to or shorter than the characteristic timescale of enzyme adsorption, and the reaction diffusion model reduces to two coupled kinetic equations, Eqs. 45 and 46, subject to conservation relations for the enzyme and the substrate, respectively. The latter equations are similar to the equations used to describe enzymatic processes in solution, which, despite their nonintegrability, have been thoroughly analyzed using the quasi-steady-state approximation (Segel, 1988; Borghans et al., 1996; Schnell and Mendoza, 1997; Schnell and Maini, 2000). We therefore used the procedure described by Borghans et al. (1996) to derive the tQSSA of Eqs. 45–48 and to obtain approximate analytical expressions for the concentration of unde-

graded collagen monomers and for the free and bound enzyme. A necessary and sufficient criterion was derived that guarantees the validity of the tQSSA, provided the enzyme concentration is either very high or very low compared to $K_M$.

The results of the first-order tQSSA were used to derive a sequential theoretical experimental method for estimating all four of the model parameters that govern the dynamics in the limit of instantaneous diffusion $\gamma$, $k_{cat}$, $K_M$, and $k_f$. This method consists of a standard equilibrium binding experiment followed by a series of degradation experiments that are analogous to the ones currently used to analyze enzymatic reactions in solution (Stryer, 1988; Ritchie and Prvan, 1996; Goudar et al., 1999; Schnell and Mendoza, 2000). The proposed parameter estimation method could not be directly tested against published experimental data. Nevertheless, partial verification of the model and the tQSSA predictions was achieved by analyzing the experiments of Welgus et al. (1980) on the erosion of fibrillar collagen by skin fibroblast collagenase. Using a priori estimates, the limit of instantaneous diffusion and the tQSSA were both shown to be at least roughly valid for the latter experiments. Moreover, using preliminary estimates of $\gamma$, $K_D$, and $k_{cat}$ enabled us, for the first time, to estimate $K_M$ for this system. These estimates were tested by using them to numerically simulate additional experiments reported by Welgus et al. (1980), such as the dependence of the rate of erosion on, respectively, the amount of enzyme solution and the thickness of the fibrillar matrix. It is noteworthy that a semiquantitative correspondence was found between simulation and experiment in both cases. The finding that $K_M$ (37°C) $<$ $K_D$ (25°C) implies that $k_r \gg k_{cat}$ at 37°C and is consistent with the corresponding values for collagen monomers in solution (Welgus et al., 1985). Moreover, it implies that $k_f$ is significantly larger than the lower bound estimate, $k_{cat}/K_M \approx 5.6 \times 10^7$ M$^{-1}$h$^{-1}$. This conclusion is consistent with the estimate $k_f = 2.4 \times 10^8$ M$^{-1}$h$^{-1}$ for skin fibroblast collagenase binding onto specific receptors on osteoblastic cells (Omura et al., 1994) and with the report by Matsushita et al. (2001) that, due to extremely fast binding kinetics, they were unable to estimate the onrate for bacterial collagenase binding onto fibrillar collagen.

Two general predictions of the first-order tQSSA are of special importance. The first is the prediction of a hyperbolic dependence of the initial rate of erosion on the total enzyme concentration ($E_0$). This result is consistent with experimental results for fibrillar collagen (Steven, 1976a,b; Welgus et al., 1980) and other insoluble proteins (Bailey and Ollis, 1977; Sattler et al., 1989; Rahmouni et al., 2001). Moreover, a definitive prediction is made regarding the apparent Michaelis–Menten constant implied by this hyperbolic relation (or double-reciprocal plot), Eq. 114, which is consistent with the experimental finding of a decreasing Michaelis–Menten constant (Sattler et al., 1989). Second, the first-order tQSSA is valid for $h^{-1}\gamma\rho_0 \ll K_M$ and

implies ideal surface erosion for this case. This is of special relevance to single thick fibrils such that $\gamma \ll 1$, and $h \gg 1$. This result is consistent with the phenomenological model proposed by Hayashi and Ikada (1990) for the enzymatic erosion of insoluble fibrils. Moreover, in the limits of high and low enzyme concentrations, respectively, results 104 and 112 provide a definitive prediction for the rate constant appearing in the model of Hayashi and Ikada (1990). Because both these conclusions are consistent with experiments using bacterial collagenase (Steven, 1976a,b; Okada et al., 1992), it seems plausible that the proposed model is at least roughly valid for these enzymes. This result may seem a bit surprising in light of the fact that, in solution, bacterial collagenase is known to cleave collagen monomers at several hyperactive sites (French et al., 1992). Nevertheless, it should be remembered that, above 34°C, cleavage of the collagen triple helix by bacterial collagenase invariably results in uncoiling of the cleaved helices (Mallya et al., 1992), which means that cleavage of the first hyperactive site is the rate-limiting process. Unfortunately, the published data on the degradation of fibrillar collagen by bacterial collagenase cannot be analyzed quantitatively because they do not give sufficient details such as matrix dimensions and concentration.

Finally, we consider the validity of the proposed model and of the corresponding tQSSA for more general situations. First, the limit of instantaneous diffusion (and hence the tQSSA) is only valid for thin sparse samples. The erosion of sparse but thick fibrillar matrices of arbitrary shape can be simulated by numerically solving Eqs. 22–33 as discussed in Numerical Methods, provided that the model parameters are given. The latter can be obtained by applying the proposed parameter estimation method to thin samples of the same composition. An additional complication that has to be considered is that the initial volume fraction of the fibrils may be significantly higher than 0.1 for certain biological tissues (Lewis and Shaw, 1997; Langsjo et al., 1999; Sung et al., 1999) and biomedical applications (Freiss et al., 1996; Fujioka et al., 1998; Sung et al., 1999). In this case, the diffusion coefficients (Ogston et al., 1976; Weadock et al., 1987; Gilbert et al., 1988) and partition coefficients (Ogston, 1958; White and Deen, 2000) of the enzyme and degradation products all depend on the volume fraction of the fibrils, and therefore vary during the erosion process. The incorporation of partitioning effects into the model equations is straightforward (Schuck, 1996), and the resulting equations can be solved numerically using the FEM used here. Moreover, the tQSSA is expected to correspond to the late asymptotic of the erosion process, provided that the time scale for enzyme diffusion is short compared to the slow degradation time scale, $t_{\bar{\rho}}$. Namely, if the enzyme diffusion coefficient is not highly nonlinear, diffusion only serves to delay enzyme adsorption and the establishment of the (homogeneous) quasi-steady state, which is manifest as an induction period in the erosion profile.

If the fibrillar matrix is extremely dense, the typical time scale for enzyme diffusion can be long compared to $t_{\bar{\rho}}$, in which case the erosion process is diffusion controlled and is well described using simple surface erosion models (Tsuk and Oster, 1961; Hayashi and Ikada, 1990). As already noted, the tQSSA of the current model can be used to describe the surface erosion of thick cylindrical fibers. This result is not surprising if we recall that the building blocks of the model are surface-eroding fibrils. Thus, the only requirement is that the density of the thick fiber should be comparable to the density of a single fibril, so that it impedes the penetration of enzyme molecules into its bulk. These considerations suggest that the enzymatic surface erosion of other simple geometries can similarly be described by the current model, with the appropriate modification of Eq. 17, which relates between the concentration of available surface binding sites, $\bar{S}$, and the concentration of monomers, $\bar{\rho}$. Finally, although we used fibrillar collagen as a concrete example, the proposed model can easily be extended to simulate the enzymatic erosion of other proteins such as cellulose (Sattler et al., 1989; Viikari et al., 1991) and cross-linked starch (Rahmouni et al., 2001). However, reservation has to be made for the fact that these substrates are in fact mixtures of two substrates with vastly different susceptibilities toward enzymatic degradation. The slowly degrading regions are fibrillar for cellulose (Viikari et al., 1991) and crystalline for cross-linked starch (Rahmouni et al., 2001). Hence, in the case of cellulose, the proposed model can probably be used to describe the erosion of the fibrillar fraction without any changes. In contrast, the consideration of semicrystalline proteins may require the derivation of a different relation between the concentration of available binding sites, $\bar{S}$, and the concentration of potential binding sites, $\bar{\rho}$. Nevertheless, the methods of analysis used in the current paper should also be applicable to the latter case.

## REFERENCES

Aharon, S., M. Bercovier, and H. Parnas. 1996. Parallel computation enables precise description of $Ca^{2+}$ distribution in nerve terminals. *Bull. Math. Biol.* 58:1075–1097.

Bailey, J. E., and D. F. Ollis. 1977. Biochemical Engineering Fundamentals. McGraw-Hill, New York.

Buckingham, E. 1914. On physically similar systems: illustrations of the use of dimensional equations. *Phys. Rev.* 4:345–376.

Bleeg, H. S. 1991. Collagenolytic enzymes assayed by spectrophotometry with suspensions of reconstituted collagen fibrils. *Connect. Tissue. Res.* 26:247–257.

Borghans, J. A. M., R. J. De Boer, and L. A. Segel. 1996. Extending the quasi-steady state approximation by changing variables. *Bull. Math. Biol.* 58:43–63.

Brilla, C. G., R. C. Funk, and H. Rupp. 2000. Lisinopril-mediated regression of mycrodial fibrosis in patients with hypertensive heart disease. *Circulation.* 102:1388–1393.

Chamberlain, L. J., I. V. Yannas, H. P. Hsu, and M. Spector. 1997. Histological response to a fully degradable collagen device implanted in a gap in the rat sciatic nerve. *Tissue Eng.* 3:353–362.

Compton, C. C., C. E. Butler, I. V. Yannas, G. Warland, and D. P. Orgill. 1998. Organized skin structure is regenerated in vivo from collagen-GAG matrices seeded with autologous keratinocytes. *J. Invest. Dermatol.* 110:908–916.

Crank, J. 1975. The Mathematics of Diffusion. Claradon Press, Oxford.

Fanti, L. A., and E. D. Glandt. 1990a. Partitioning of spherical particles into fibrous matrices. 1. Density functional theory. *J. Colloid. Sci.* 135:385–395.

Fanti, L. A., and E. D. Glandt. 1990b. Partitioning of spherical particles into fibrous matrices. 2. Monte-Carlo simulation. *J. Colloid. Sci.* 135: 396–404.

FIDAP. 1993. Theoretical Manual, edition 7.0. FDI, Evanston, IL.

Freiss, W. 1998. Collagen—biomaterial for drug delivery. *Eur. J. Pharm. Biopharm.* 45:113–136.

Freiss, W., G. Lee, and M. J. Groves. 1996. Insoluble collagen matrices for prolonged delivery of proteins. *Pharm. Dev. Tech.* 1:185–193.

French, M. F., A. Bhown, and H. E. Van Wart. 1992. Identification of *Clostridium histolyticum* collagenase hyperactive sites in type I, II and III collagens: lack of correlation with local triple helical stability. *J. Protein. Chem.* 11:83–97.

Freyman, T. M., I. V. Yannas, and L. J. Gibson. 2001. Cellular materials as porous scaffolds for tissue engineering. *Prog. Mater. Sci.* 46:273–282.

Fujioka, K., M. Maeda, T. Hojo, and A. Sano. 1998. Protein release from collagen matrices. *Adv. Drug Del. Rev.* 31:247–266.

Gilbert, D., and S. W. Kim. 1990. Macromolecular release from collagen monolithic devices. *J. Biomed. Mater. Res.* 24:1221–1239.

Gilbert, D., T. Okano, T. Miyata, and S. W. Kim. 1988. Macromolecular diffusion through collagen membranes. *Int. J. Pharm.* 47:79–88.

Goudar, C. T., J. R. Sonnad, and R. G. Duggleby. 1999. Parameter estimation using a direct solution of the integrated Michaelis–Menten equation. *Biochim. Biophys. Acta.* 1429:377–383.

Hasty, K., J. J. Jeffrey, M. S. Hibbs, and H. G. Welgus. 1987. The collagen substrate specificity of human neutrophil collagenase. *J. Biol. Chem.* 262:10048–10052.

Hayashi, T., and Y. Ikada. 1990. Enzymatic hydrolysis of copoly-(*n*-hydroxyalkyl L-glutamine/γ-methyl L glutamate) fibers. *Biomaterials.* 11:409–412.

Hughes, T. J. R. 1987. The Finite Element Method. Prentice-Hall, Englewood Cliffs, New Jersey.

Hulmes, D. J. S., T. J. Wess, D. J. Prockop, and P. Fratzl. 1995. Radial packing, order and disorder in collagen fibrils. *Biophys. J.* 68: 1661–1670.

Kadler, K. E., D. F. Holmes, J. A. Trotter, and J. A. Chapman. Collagen fibril formation. 1996. *Biochem. J.* 316:1–11.

Langsjo, T. K., M. Hyttinen, A. Pelttari, K. Kiraly, J. Arokoski, and H. J. Helminen. 1999. Electron microscopic stereological study of collagen fibrils in bovine articular cartilage: volume and surface densities are best obtained indirectly (from length densities and diameters) using isotropic uniform random sampling. *J. Anat.* 195:281–293.

Lapiere, C. M., and J. Gross. 1963. Animal collagenase and collagen metabolism. *In* Mechanisms of Hard Tissue Destruction, Vol. 75. R. F. Sognnaes, editor. American Association for the Advancement of Science, Washington, DC. 663–694.

Letnam, M. C. 1951. Adsorption. McGraw-Hill, New York.

Lewis, G., and K. M. Shaw. 1997. Modeling the tensile behavior of human Achilles tendon. *Biomed. Mater. Eng.* 7:231–244.

Li, S. T. 1995. Biological biomaterials: tissue derived biomaterials. *In* The Biomedical Engineering Handbook. J. D. Bronzino, editor. CRC Press Inc. in cooperation with IEEE Press, Boca Racon, FL. 627–647.

Lin, C. C., and L. A. Segel. 1974. Mathematics Applied to Deterministic Problems in the Natural Sciences. Chap. 6. MacMillan, New York.

Lin, H. D., O. Clegg, and R. Lal. 1999. Real time proteolysis of single collagen I molecules with atomic force microscopy. *Biochemistry*. 38:9956–9963.

Mallya, S. K., K. A. Mookhtiar, and H. E. Van Wart. 1992. Kinetics of hydrolysis of type I, II, and III collagens by class I and II *Clostridium histolyticum collagenases*. *J. Protein Chem*. 11:99–107.

Marquardt, D. W. 1963. An algorithm for least squares estimation for nonlinear parameters. *SIAM J*. 11:431–441.

Matsushita, O., C. M. Jung, J. Minami, S. Katayama, N. Nishi, and K. Okabe. 1998. A study of the collagen binding domain of a 116-kDa *Clostridium histolyticum* class I collagenase. *J. Biol. Chem*. 273:3643–3648.

Matsushita, O., T. Koide, R. Kobayashi, K. Nagata, and A. Okabe. 2001. Substrate recognition by the collagen-binding domain of *Clostridium histolyticum* class I collagenase. *J. Biol. Chem*. 276:8761–8770.

Nimni, M. E. 1995. Collagen: molecular structure and biomaterial properties. Part A: Materials. *In* Encyclopedic Handbook of Biomaterials and Bioengineering. D. L. Wise, editor. Marcel Dekker Inc., New York. 1229–1243.

Ogston, A. G. 1958. The spaces in a uniform random suspension of fibers. *Trans. Faraday Soc*. 54:1754–1757.

Ogston, A. G., B. N. Preston, and J. D. Wells. 1976. On the transport of compact particles through solutions of chain polymers. *Proc. R. Soc. Lond. A*. 333:297–316.

Okada, T., T. Hayashi, and Y. Ikada. 1992. Degradation of collagen suture in vitro. *Biomaterials*. 13:448–454.

Omura, T. H., A. Noguchi, C. A. Johanns, J. J. Jeffrey, and N. C. Partridge. 1994. Identification of a specific receptor for interstitial collagenase on osteoblastic cells. *J. Biol. Chem*. 269:24994–24998.

Peppas, N. A., and C. T. Reinhart. 1984. Solute diffusion in swollen membranes. Part I. A new theory. *J. Membrane Sci*. 18:214–226.

Piez, K. A. 1985. Collagen. *In* Encyclopedia of Polymer Science. Vol. 3. J. I. Kroscwitz, editor. Wiley Interscience Publication, New York. 699–727.

Rahmouni, M., F. Choinard, F. Nekka, V. Lenaerts, and J. C. Leroux. 2001. Enzymatic degradation of cross-linked high amylose starch tablets and its effect on in vitro release of sodium diclofenac. *Eur. J. Pharm. Biopharm*. 51:191–198.

Riesle, J., A. P. Hollander, R. Langer, L. E. Freed, and G. Vunjak-Novakivic. 1998. Collagen in tissue-engineered cartilage: types, structure and crosslinks. *J. Cell. Biochem*. 71:313–327.

Ritchie, R. J., and T. Prvan. 1996. A simulation study on designing experiments to measure the $K_M$ of Michaelis–Menten kinetic curves. *J. Theor. Biol*. 178:239–254.

Sabelman, E. E. 1985. Biology, biotechnology and biocompatibility of collagen. *In* Biocompatibility of Tissue Analogs. D. F. Williams, editor. CRC Press, Boca Raton, FL. 27–66.

Sakai, T., and J. Gross. 1967. Some properties of the products of reaction of tadpole collagenase with collagen. *Biochemistry*. 6:518–527.

Saltzman, W. M., M. L. Randomsky, K. J. Whaley, and R. A. Cone. 1994. *Biophys. J*. 66:508–515.

Sattler, W., E. Esterbauer, O. Glatter, and W. Steiner. 1989. The effect of enzyme concentration on the rate of hydrolysis of cellulose. *Biotechnol. Bioeng*. 33:1221–1234.

Schnell, S., and P. K. Maini. 2000. Enzyme kinetics at high enzyme concentrations. *Bull. Math. Biol*. 62:483–499.

Schnell, S., and C. Mendoza. 1997. Closed form solution for time-dependent enzyme kinetics. *J. Theor. Biol*. 187:207–212.

Schuck, P. 1996. Kinetics of ligand binding to receptor immobilized in a polymer matrix, as detected with an evanescent wave biosensor. I. A computer simulation of the influence of mass transport. *Biophys. J*. 70:1230–1249.

Segel, L. A. 1988. On the validity of the steady state assumption of enzyme kinetics. *Bull. Math. Biol*. 50:579–593.

Shampine, L. F., and M. W. Reichlet. 1997. The Matlab ODE suite. *SIAM J. Sci. Computing*. 18:1–22.

Steven, F. S. 1976a. Observations on the different substrate behavior of tropocollagen molecules in solution and intermolecularly cross-linked tropocollagen within insoluble polymeric collagen fibrils. *Biochem. J*. 155:391–400.

Steven, F. S. 1976b. Polymeric collagen fibrils. An example of substrate-mediated steric obstruction of enzymic digestion. *Biochim. Biophys. Acta*. 452:151–160.

Stryer, L. 1988. Biochemistry. Freeman and Company, New York. 177–200.

Suga, K., G. van Dedem, and M. Moo-Young. 1975. Enzymatic breakdown of water insoluble substrates. *Biotech. Bioeng*. 17:185–201.

Sung, H. W., Y. Chang, C. T. Chiu, C. N. Chen, and H. C. Liang. 1999. Crosslinking characteristics and mechanical properties of bovine pericardium fixed with naturally occurring crosslinking agent. *J. Biomed. Mater. Res*. 47:116–126.

Sung, H. W., C. S. Hsu, S. P. Wang, and H. L. Hsu. 1997. Degradation potential of biological tissue fixed with various fixatives: an in vitro study. *J. Biomed. Mater. Res*. 34:147–155.

Tsuk, A. G., and G. Oster. 1961. Determination of enzyme activity by a linear measurement. *Nature*. 190:721–722.

Tyn, M. T., and T. W. Gusek. 1990. Prediction of diffusion coefficients of proteins. *Biotech. Bioeng*. 35:327–338.

Tzafriri, A. R. 2000. Mathematical modeling of diffusion mediated release from bulk degrading matrices. *J. Control Rel*. 63:69–79.

Van Wachem, P. B., J. A. Plantinga, M. J. B. Wisink, R. Beernink, A. A. Poot, G. H. M. Engbers, T. Beugeling, W. G. van Aken, J. Feijen, and M. J. A. van Luyn. 2001. In vivo biocompatibility of carbodiimide-crosslinked collagen matrices: effect of cross-linking density, heparin immobilization, and bFGF loading. *J. Biomed. Mater. Res*. 55:368–378.

Van Wart, H. E., and D. R. Steinbrink. 1985. Complementary substrate specificities of class I and class II collagenases from *Clostridium histolyticum. Biochemistry*. 24:6520–6526.

Viikari, L., A. Kantelinen, M. Ratto, and J. Sundquist. 1991. Enzymes in pulp and paper processing. *In* ACS Symposium Series no. 460. G. F. Leatham and M. E. Himmel, editors. ACS, Washington, DC.

Weadock, K. S., D. Wolff, and F. H. Silver. 1987. Diffusivity of ^{125}I-labelled macromolecules through collagen: mechanism of diffusion and effect of adsorption. *Biomaterials*. 8:105–112.

Welgus, H. G., J. J. Jeffrey, and A. Z. Eisen. 1981a. The collagen substrate specificity of human skin fibroblast collagenase. *J. Biol. Chem*. 256:9511–9516.

Welgus, H. G., J. J. Jeffrey, and A. Z. Eisen. 1981b. Human skin fibroblast collagenase. *J. Biol. Chem*. 256:9516–9521.

Welgus, H. G., J. J. Jeffrey, A. Z. Eisen, W. T. Roswit, and G. P. Stricklin. 1986. Human skin fibroblast collagenase: interaction with substrate and inhibitor. *Coll. Relat. Res*. 5:167–179.

Welgus, H. G., J. J. Jeffrey, G. P. Stricklin, and A. Z. Eisen. 1982. The gelatinolytic activity of human skin fibroblast collagenase. *J. Biol. Chem*. 257:11534–11539.

Welgus, H. G., J. J. Jeffrey, G. P. Stricklin, W. T. Roswit, and A. Z. Eisen. 1980. Characteristics of the action of human skin fibroblast collagenase on fibrillar collagen. *J. Biol. Chem*. 255:6806–6813.

White, J. A., and W. M. Deen. 2000. Equilibrium partitioning of flexible macromolecules in fibrous membranes and gels. *Macromolecules*. 33:8504–8511.

Wissink, M. J. B., R. Beernink, A. A. Poot, G. H. M. Enbers, T. Beugeling, W. G. van Aken, and J. Feijen. 2000. Improved endothelialization of vascular grafts by local release of growth factor from heparinized collagen matrices. *J. Control Rel*. 64:103–114.

Wu, H., M. H. Byrne, A. Stacey, M. B. Goldring, J. R. Birkhead, R. Jaenisch, and S. M. Krane. 1990. Generation of collagenase-resistant collagen by site directed mutagenessis of murine proα(I) collagen gene. *Proc. Natl. Acad. Sci. U.S.A*. 87:5888–5892.

Zhu, K. Y., T. Umino, X. D. Liu, H. J. Wang, D. J. Rosenberger, J. R. Spurzem, and S. I. Rennard. 2001. Contraction of fibroblast containing collagen gels: initial collagen concentration regulates the degree of contraction and cell survival. *In Vitro Cell Dev. An*. 37:10–16.